Database for drug metabolism and comparisons, NICEdrug.ch, aids discovery and design

Authors/affiliation

Homa MohammadiPeyhani[1], Anush Chiappino-Pepe[1,2,5], Kiandokht Haddadi[1,3,5], Jasmin Hafner[1], Noushin Hadadi[1,4], Vassily Hatzimanikatis[1,*]

[1]Laboratory of Computational Systems Biotechnology, École Polytechnique Fédérale de Lausanne, EPFL, Lausanne, Switzerland

[2]Present address: Department of Genetics, Harvard Medical School, Boston, Massachusetts, USA

[3]Present address: Department of Chemical Engineering and Applied Chemistry, University of Toronto, Toronto, Canada

[4]Present address: Department of Cell Physiology and Metabolism, Université de Genève, Geneva, Switzerland

[5]These authors contributed equally

[*]Corresponding author:

Prof. Vassily Hatzimanikatis

Laboratory of Computational Systems Biotechnology (LCSB), École Polytechnique Fédérale de Lausanne (EPFL), CH-1015

Lausanne, Switzerland

Email: vassily.hatzimanikatis@epfl.ch , Phone: +41 (0)21 693 98 70, Fax: +41 (0)21 693 98 75

Abstract

The discovery of a drug requires over a decade of enormous research and financial investments—and still has a high risk of failure. To reduce this burden, we developed the NICEdrug.ch database, which incorporates 250,000 bio-active molecules, and studied their metabolic targets, fate, and toxicity. NICEdrug.ch includes a unique fingerprint that identifies reactive similarities between drug-drug and drug-metabolite pairs. We use NICEdrug.ch to evaluate inhibition and toxicity by the anticancer drug 5-fluorouracil, and suggest avenues to alleviate its side effects. Clustering based on this fingerprint in statins identified drugs for repurposing. We propose shikimate 3-phosphate for targeting liver-stage malaria with

minimal impact on the human host cell. Finally, NICEdrug.ch suggests over 1,300 drugs and food molecules to target COVID-19 and explains their inhibitory mechanisms. The NICEdrug.ch database is accessible online to systematically identify the reactivity of small molecules and druggable enzymes with practical applications in lead discovery and drug repurposing.

Keywords

Ligand-based drug discovery, drug clustering, drug metabolic fate, prodrug, drug similarity, drug toxicity, drug side effects, reactive site similarity, enzyme inhibition, nutraceuticals.

Introduction

To assure effective therapies for previously untreated illness, emerging diseases, and personalized medicine, new small molecules are always needed. However, the process to develop new drugs is complex, costly, and time consuming. This is especially problematic considering about 90% of drug candidates in clinical trials are discarded due to unexpected toxicity or other secondary effects. This inefficiency threatens our health care system and economy (Wong et al., 2019). Improving how we discover and design new drugs could reduce the time and costs involved in the developmental pipeline and hence is of primary importance to define efficient medical therapies.

Current drug discovery techniques often involve high-throughput screens with candidates and a set of target enzymes presumably involved in a disease, which leads to the selection for those candidates with the preferred activity. However, the biochemical space of small molecules and possible targets in the cell is huge, which limits the possible experimental testing. Computational methods for drug pre-screening and discovery are therefore promising. *In silico,* one can systematically search the maximum biochemical space for targets and molecules with desired structures and functions to narrow down the molecules to test experimentally.

There are two main *in silico* strategies for drug discovery: a data-driven approach based on machine learning, or a mechanistic approach based on the available biochemical knowledge. Machine learning (ML) has been successfully used in all stages of drug discovery, from the

prediction of targets to the discovery of drug candidates, as shown in some recent studies (Shilo et al., 2020; Stokes et al., 2020; Vamathevan et al., 2019). However, ML approaches require big, high-quality data sets of drug activity and associated physiology (Vamathevan et al., 2019), which might be challenging to obtain when studying drug action mechanisms and side effects in humans. ML also uses trained neural networks, which can lack interpretability and repeatability. This can make it difficult to explain why the neural networks has chosen a specific result, why it unexpectedly failed for an unseen dataset, and the final results may vary (Vamathevan et al., 2019).

Mechanistic-based approaches can also rationally identify small molecules in a desired system and do not require such large amounts of data. Such methods commonly screen based on structural similarity to a native enzyme substrate (antimetabolite) or to a known drug (for drug repurposing), considering the complete structure of a molecule to extract information about protein-ligand fitness (Jarvis and Ouvry, 2019; Verlinde and Hol, 1994). However, respecting enzymatic catalysis, the reactive sites and neighboring atoms play a more important role than the rest of the molecule when assessing molecular reactivity (Hadadi et al., 2019). Indeed, reactive site-centric information might allow to identify: (1) the metabolic fate and neighbors of a small molecule (Javdan et al., 2020), including metabolic precursors or prodrugs and products of metabolic degradation, (2) small molecules sharing reactivity (Lim et al., 2010), and (3) competitively inhibited enzymes (Ghattas et al., 2016). Furthermore, neither ML nor mechanistic-based approaches consider the metabolism of the patient, even though the metabolic fate of the drug and the existence of additional targets in the cell might give rise to toxicity. To our knowledge, no available method accounts for human biochemistry when refining the search for drugs.

In this study, we present the development of the NICEdrug.ch database using a more holistic and updated approach to a traditional mechanistic-based screen by (1) adding a more detailed analysis of drug molecular structures and target enzymes based on structural aspects of enzymatic catalysis and (2) accounting for drug metabolism in the context of human biochemistry. NICEdrug.ch assesses the similarity of the reactivity between a drug candidate and a native substrate of an enzyme based on their common reactive sites and neighboring atoms (i.e., the NICEdrug score) in an analogous fashion as the computational tool BridgIT

(Hadadi et al., 2019). It also identifies all biochemical transformations in the cellular metabolism that can modify and degrade a drug candidate using a previously developed reaction prediction tool, termed BIochemical Network Integrated Computational Explorer (BNICE.ch) (Hatzimanikatis et al., 2005; Soh and Hatzimanikatis, 2010) and the ATLAS of Biochemistry (Hadadi et al., 2016; Hafner et al., 2020). With NICEdrug.ch, we automatically analyzed the functional, reactive, and physicochemical properties of around 250,000 small molecules to suggest the action mechanism, metabolic fate, toxicity, and possibility of drug repurposing for each compound. We apply NICEdrug.ch to study drug action mechanisms and identify drugs for repurposing related to four diseases: cancer, high cholesterol, malaria, and COVID-19. We also sought for molecules in food, as available in fooDB the largest database of food constituents (Scalbert et al., 2011), with putative anti SARS-CoV-2 activity. Finally, we provide NICEdrug.ch as an online resource (https://lcsb-databases.epfl.ch/pathways/Nicedrug/). Overall, NICEdrug.ch combines knowledge of molecular structures, enzymatic reaction mechanisms (as included in BNICE.ch (Finley et al., 2009; Hadadi and Hatzimanikatis, 2015; Hatzimanikatis et al., 2005; Henry et al., 2010; Soh and Hatzimanikatis, 2010; Tokic et al., 2018)), and cellular biochemistry (currently human, *Plasmodium*, and *Escherichia coli* metabolism) to provide a promising and innovative resource to accelerate the discovery and design of novel drugs.

Results

Discovery of 200,000 bioactive molecules one reaction away from known drugs in a human cell for analysis of drug metabolism with NICEdrug.ch

To build the initial NICEdrug.ch database, we gathered over 70,000 existing small molecules presumed suitable for treating human diseases from three source databases: KEGG, ChEMBL, and DrugBank (Figure S1, Materials and Methods). We eliminated duplicate molecules, curated available information, computed thermodynamic properties, and applied the Lipinski rules (Lipinski et al., 2001) to keep only the molecules that have drug-like properties in NICEdrug.ch (Figure 1, Materials and Methods). NICEdrug.ch currently includes 48,544 unique small molecules from the source databases.

To evaluate the reactivity of the 48,544 drugs, we searched for all possible reactive sites on each drug with BNICE.ch (Hatzimanikatis et al., 2005) (Figure 1, Materials and Methods). All

of the 48,544 drugs contain at least one reactive site and hence might be reactive in a cell. In total, we identified more than 5 million potential reactive sites (183k unique) on the 48,544 molecules and matched them to a corresponding enzyme by assigning them to an Enzyme Commission (E.C.) number. All of these enzymes belong to the human metabolic network (Table S1, Materials and Methods). Interestingly, 10.4% of identified reactive sites correspond to the p450 class of enzymes, which are responsible for breaking down compounds in the human body by introducing reactive groups on those compounds, also known as phase I of drug metabolism (Figure S2A). The sites that were identified varied greatly from simple and small (i.e., comprising a minimum number of one atom) to more complex sites that covered a large part of the molecule. The biggest reactive site includes 30 atoms (Figure S2B).

Given the important role of metabolism in the biochemical transformations and toxicity of drugs, we investigated the metabolism of the 48,544 input molecules in human cells. We predicted the hypothetical biochemical neighborhoods of all NICEdrug.ch small molecules in a human cell (i.e., reacting with known human metabolites and cofactors) using a retro-biosynthetic analysis with BNICE.ch (Figure 1, Table S1, Materials and Methods). With this approach, we discovered 197,246 unique compounds connected to the input drugs via one step or reaction (products of the first generation), and the associated hypothetical biochemical neighborhood consists of 630,449 reactions (Figure S2). The 197,246 unique compounds are part of a new set of bioactive molecules in NICEdrug.ch that might act as drugs or prodrugs in a human cell. We stored the total number of 245,790 small molecules (including the curated set of 48,544 drugs and the new set of 197,246 bioactive compounds), their calculated properties, and biochemistry in our open-access database of drug metabolism, NICEdrug.ch.

To use NICEdrug.ch to identify drug-drug or drug-metabolite pairs that have shared reactivity and target enzymes, we developed a new metric called the *NICEdrug score* (Figure S3). The NICEdrug score uses information about the structure of the reactive site and its surroundings (as computed using the BridgIT methodology) and is stored in the form of a fingerprint (Materials and Methods). The fingerprint of a molecule's reactive site and the neighborhood around this reactive site—termed the *reactive site-centric fingerprint*—serves to compare this

site-specific similarity with other molecules. We recently showed that the reactive site-centric fingerprint of a reaction provides a better predictive measure of similar reactivity than the overall molecular structure, as the overall structure can be much larger than the reactive site and skew the results by indicating high similarities when the reactivity is actually quite different (Hadadi et al., 2019). Here, we generated reactive site-centric fingerprints for all 20 million reactive sites identified in the 48,544 drugs and 197,246 one-step-away molecules included in NICEdrug.ch. The 20 million reactive site-centric fingerprints for the total 245,790 small molecules are available in NICEdrug.ch to be used in similarity comparisons and classifying molecules (Materials and Methods).

We propose the usage of NICEdrug.ch to generate reports that define the hypothetical reactivity of a molecule, the molecule's reactive sites as identified by target enzymes, and the NICEdrug score between drug-drug and drug-metabolite pairs. The NICEdrug.ch reports can be used for three main applications: (1) to identify the metabolism of small molecules; (2) to suggest drug repurposing; and (3) to evaluate the druggability of an enzyme in a desired cell or organism (Figure 1), as we show in the next sections. Currently, NICEdrug.ch includes metabolic information for human cells, a malaria parasite, and *Escherichia coli*, and it is easily extendible to other organisms in the future.

NICEdrug.ch suggests inhibitory mechanisms of the anticancer drug 5-FU and avenues to alleviate its toxicity.

As a case study, we used NICEdrug.ch to investigate the mode of action and metabolic fate of one of the most commonly used drugs to treat cancer, 5-fluorouracil (5-FU), by exploring its reactivity and the downstream products or intermediates that are formed during the cascade of biochemical transformations. 5-FU interferes with DNA synthesis as an antimetabolite (Longley et al., 2003), meaning that its various intermediates like 5-fluorodeoxyuridine monophosphate (FdUMP) are similar enough to naturally occurring substrates and they can act as competitive inhibitors in the cell.

We therefore used NICEdrug.ch to study the intermediates of 5-FU that occurred between one to four reaction steps away from 5-FU (Table S2), which is a reasonable range to occur in the body after 5-FU treatment (Testa, 2010). This analysis identified 407 compounds (90

biochemical and 317 chemical molecules) that have the biochemical potential to inhibit certain enzymes. Because the NICEdrug score that analyses reactive site and neighborhood similarities can serve as a better predictor of metabolite similarity, we assessed the NICEdrug score of the intermediates compared to human metabolites. This resulted in a wide range of NICEdrug scores between the different 5-FU intermediates and human metabolites, ranging from no similarity at a NICEdrug score of 0 to the equivalent substructure on a compound at a NICEdrug score of 1. More importantly, some of the 407 metabolite inhibitors (as explained next) were known compounds that have been investigated for their effects on 5-FU toxicity, but most of these compounds were newly identified by NICEdrug.ch and could therefore serve as avenues for future research into alleviating the side effects of this drug.

We investigated these 407 compounds in more detail, looking first at the set of already validated metabolite inhibitors. 5-Fluorouridine (two steps away from 5-FU) and UDP-L-arabinofuranose (four steps away from 5-FU) are very similar to uridine, with NICEdrug scores of 0.95 and 1, respectively. Uridine is recognized as a substrate by two human enzymes, cytidine deaminase (EC: 3.5.4.5) and 5'-nucleotidase (EC: 3.1.3.5) (Figure 2). Therefore, NICEdrug.ch predictions show that the degradation metabolism of 5-FU generates downstream molecules similar to uridine, which likely leads to the inhibition of these two enzymes. This effect has already been investigated as a potential method for reducing the toxicity of 5-FU, wherein it was proposed that high concentrations of uridine could compete with the toxic 5-FU metabolites (Ma et al., 2017).

NICEdrug.ch also identified a few potential metabolites that have not been previously studied for their effects. These metabolites share a reactive site with native human metabolites and differ in the reactive site neighborhood, and we refer to them as *para-metabolites* (Sartorelli and Johns, 2013). 6-Methyl-2'-deoxyadenosine, purine-deoxyribonucleoside, and 2'-deoxyisoguanosine structurally resemble the reactive site neighborhood of deoxyadenosine, with respective NICEdrug scores of 1, 1, and 0.91. Similarly, 2-aminoadenosine, 2-chloroadenosine, and 2-methylaminoadenosine (four steps from 5-FU) have the same reactive site neighborhood as adenosine, with NICEdrug scores of 1, 1, and 0.96, respectively. Adenosine and deoxyadenosine are both native substrates of the adenosine kinase (EC: 2.7.1.20) and 5'-nucleotidase (EC: 3.1.3.5) (Figure 2). Therefore, we suggest that the 5-FU

derivatives 2-aminoadenosine and 2-chloroadenosine are competitive inhibitors for the two enzymes adenosine kinase and 5'-nucleotidase. With these new insights from NICEdrug.ch, we hypothesize that co-administering adenosine or deoxyadenosine and uridine (Figure 2) with 5-FU might be required to reduce its toxic effects and hopefully alleviate the side effects of the 5-FU cancer treatment.

Metabolic degradation of 5-FU leads to compounds with Fluor in their reactive site that are less reactive and more toxic than other intermediates.

In the previous case study, we showed inhibitors that contain the identical active site to the native enzyme. However, a slightly different reactive site might still be able to bind to an enzyme and compete with a native substrate, also defined as *anti-metabolite* (Matsuda et al., 2014). We explored this scenario by defining relaxed constraints in two steps. We first identified all atoms around a reactive site to compare the binding characteristics between the native molecule and putative inhibitor. Next, we compared the reactive site of the native molecule and putative inhibitor and scored the latter based on similarity (Materials and Methods). Following these two steps, we assessed the similarity between intermediates in the 5-FU metabolic neighborhood and human metabolites. Among all 407 compounds in the 5-FU metabolism (Table S2), we found 8 that show a close similarity to human metabolites (NICEdrug score above 0.9, Figure 3) that might be competitive inhibitors or anti-metabolites. Inside the reactive site, the original hydrogen atom is bioisosterically replaced by fluorine. F-C bonds are extremely stable and therefore block the active site by forming a stable complex with the enzyme. The inhibitory effect of the intermediates tegafur, 5-fluorodeoxyuridine, and F-dUMP (one to two reaction steps away) has been confirmed in studies by Kobayakawa et.al (Kobayakawa and Kojima, 2011) and Bielas et.al (Bielas et al., 2009). In addition, NICEdrug.ch also predicts that 5flurim, 5-fluorodeoxyuridine triphosphate, 5-fluorodeoxyuridine triphosphate, 5-fluorouridine diphosphate, and 5-fluorouridine triphosphate, some of which occur further downstream in the 5-FU metabolism, also act as antimetabolites (Figure 3). Based on the insights from NICEdrug.ch, we suggest the inhibitory and side effect of 5-FU treatment might be more complex than previously thought. 5-FU downstream products are structurally close to human metabolites and might form stable complexes with native enzymes. This knowledge could serve to further refine the

256 pharmacokinetic and pharmacodynamic models of 5-FU and ultimately the dosage
257 administered during treatment.
258
259 ***NICEdrug.ch identifies toxic alerts in the anticancer drug 5-FU and its products from***
260 ***metabolic degradation.***
261 The concept of drug toxicity refers not to overdoses but instead to the toxic effects at medical
262 doses (Guengerich, 2011), which often occur due to the degradation products generated
263 through drug metabolism. Extensive efforts have been expended to identify toxic molecules
264 or, more generally, to extract the substructures that are responsible for toxicity (called
265 structural alerts). The Liver Toxicity Knowledge Base (LTKB) and the super toxic database
266 include 1,036 and about 60k toxic molecules, respectively (Schmidt et al., 2009; Thakkar et
267 al., 2018). ToxAlert provides around 1,200 alerts related to different forms of toxicity (Sushko
268 et al., 2012). However, the number of molecules that are analyzed and labeled as toxic in
269 databases is disproportionally low compared to the space of compounds. Additionally,
270 structural alerts are indicated for many compounds, and current alerts might identify
271 redundant and over-specific substructures, which questions their reliability (Yang et al.,
272 2017).
273
274 To quantify the toxicity of downstream products of drugs in NICEdrug.ch, we collected all of
275 the molecules cataloged as toxic in the LTKB and super toxic databases (approved toxic
276 molecules) along with their lethal dose (LC_{50}), as well as the existing structural alerts provided
277 by ToxAlert. We measured the similarity of an input molecule with all approved toxic
278 molecules using the reactive site-centric fingerprints implemented in BridgIT and the
279 NICEdrug score (Materials and Methods). Next, we scanned both the toxic reference molecule
280 and the input molecule for structural hints of toxicity, referred to here as *NICEdrug toxic*
281 *alerts*. We kept common NICEdrug toxic alerts between the reference, which is a confirmed
282 toxic compound, and input molecule. With this procedure in place, NICEdrug.ch finds for each
283 input molecule the most similar toxic molecules along with their common toxic alerts and
284 serves to assess the toxicity of a new molecule based on the mapped toxic alerts. Additionally,
285 the NICEdrug toxic alerts and toxicity level of drug intermediates can be traced with
286 NICEdrug.ch through the whole degradation pathway to reveal the origin of the toxicity.
287

288 As an example, we herein tested the ability of NICEdrug.ch to identify the toxicity in 5-FU
289 metabolism. First, we queried the toxicity profile of all intermediates in the 5-FU metabolic
290 neighborhood, integrating both known and hypothetical human reactions (Materials and
291 Methods). In this analysis, we generated all compounds up to four steps away from 5-FU.
292 Based on the toxicity report of each potential degradation product, we calculated a relative
293 toxicity metric that adds the LC_{50} value, NICEdrug score, and number of common NICEdrug
294 toxic alerts with all approved toxic drugs (Materials and Methods). We generated the
295 metabolic neighborhood around 5-FU, and labeled each compound with our toxicity metric
296 (Table S2). Interestingly, we show that the top most toxic intermediates match the list of
297 known three toxic intermediates in 5-FU metabolism (Figure 4) (Krauß and Bracher, 2018).
298 Based on the toxicity analysis in NICEdrug.ch for 5-FU, we hypothesize there are highly toxic
299 products of 5-FU drug metabolism that had not been identified either experimentally or
300 computationally and it might be necessary to experimentally evaluate their toxicity to
301 recalibrate the dosage of 5-FU treatment.
302

303 ***The NICEdrug reactive site-centric fingerprint accurately clusters statins of type I and II***
304 ***and guides drug repurposing.***

305 Because potential side effects of a drug are documented when the drug passes the approval
306 process, repurposing approved drugs for other diseases can reduce the medical risks and
307 development expenses. For instance, the antitussive noscapine has been repurposed to treat
308 some cancers (Mahmoudian and Rahimi-Moghaddam, 2009; Rajesh, A. and International,
309 2011). Because NICEdrug.ch can search for functional (i.e., reactivity), structural (i.e., size),
310 and physicochemical (i.e., solubility) similarities between molecules while accounting for
311 human biochemistry, we wanted to determine if NICEdrug.ch could therefore suggest drug
312 repurposing strategies.
313

314 As a case study, we investigated the possibility of drug repurposing to replace statins, which
315 are a class of drugs often prescribed to lower blood cholesterol levels and to treat
316 cardiovascular disease. Indeed, data from the National Health and Nutrition Examination
317 Survey indicate that nearly half of adults 75 years and older in the United States use
318 prescription cholesterol-lowering statins (US Preventive Services Task Force, 2016). Since
319 some patients do not tolerate these drugs and many still do not reach a safe blood cholesterol

level (Kong et al., 2004), there is a need for alternatives. Being competitive inhibitors of the cholesterol biosynthesis enzyme 3-hydroxy-3-methyl-glutaryl-coenzyme A reductase (HMG-CoA reductase) (Jiang et al., 2018; Mulhaupt et al., 2003), all statins share the same reactive site. BNICE.ch labeled this reactive site, in a linear or circular form, as corresponding to an EC number of 4.2.1.- (Istvan, 2001). NICEdrug.ch includes 254 molecules with the same reactive site that are recognized by enzymes of E.C. class 4.2.1.-, ten of which are known statins. We used the NICEdrug score to cluster the 254 molecules into different classes (Table S3, Figure 5). Two of the classes correspond to all currently known statins, which are classified based on their activity into type 1 and 2, wherein statins of type 2 are less active and their reactive site is more stable compared to type 1. This property is well distinguished in the clustering based on the NICEdrug score (Figure 5A).

In addition to properly classifying the ten known statins (Figure 5B and 5C, molecules non-marked), we identified seven other NICEdrug.ch molecules that clustered tightly with these statins (Figure 5B and 5C, molecules marked with *). These new molecules share the same reactive site and physicochemical properties, and they have the highest similarity with known statins in atoms neighboring the reactive site. In a previous study by Endo *et al.*, these seven NICEdrug.ch molecules were introduced as Mevastatin analogues for inhibiting cholesterol biosynthesis (Endo and Hasumi, 1993). Therefore, they were already suggested as possible candidates for treating high blood cholesterol and could be a good option for repurposing. Furthermore, we found eight known drugs not from the statin family among the 254 scanned molecules (Table S4). One of them, acetyl-L-carnitine (Figure 5C, molecule marked with **), is mainly used for treating neuropathic pain (Li et al., 2015), though Tanaka *et al.* have already confirmed that it also has a cholesterol-reducing effect (Tanaka et al., 2004).

Overall, NICEdrug.ch was able to characterize all known enzymatic reactions that metabolize statins, including proposed alternatives and new hypothetical reactions that could be involved in their metabolism within human cells (Figure 5A, Figure S4). The identification of seven drugs that clustered around the statins and were already designed as alternatives to statins verifies the ability of NICEdrug.ch and the NICEdrug score to search broad databases for similar compounds in structure and function. Furthermore, the discovery of the eight compounds unrelated to known statins offer multiple candidate repurposable drugs along

352 with a map of their metabolized intermediates for the treatment of high cholesterol, though
353 further preclinical experiments would be required to verify their clinical benefits.
354
355 ***NICEdrug.ch suggests over 500 drugs to target liver-stage malaria and simultaneously***
356 ***minimize side effects in human cells, with shikimate 3-phosphate as a top candidate***
357 Efficiently targeting malaria remains a global health challenge. Malaria parasites
358 (*Plasmodium*) are developing resistance to all known drugs, and antimalarials cause many
359 side effects (World Health Organization, 2018). We applied NICEdrug.ch to identify drug
360 candidates that target liver-stage developing malaria parasites and lessen or avoid side effects
361 in human cells.
362
363 We previously reported 178 essential genes and enzymes for liver-stage development in the
364 malaria parasite *Plasmodium berghei* (Stanway et al., 2019) (Table S5, STAR Methods). Out of
365 178 essential *Plasmodium* enzymes, 32 enzymes are not essential in human cells (Wang et al.,
366 2015) (Table S5, STAR Methods). We extracted all molecules catalyzed by these 32 enzymes
367 uniquely essential in *Plasmodium*, which resulted in 68 metabolites and 157 unique
368 metabolite-enzyme pairs (Table S5, STAR Methods). We used NICEdrug.ch to examine the
369 druggability of the 32 essential *Plasmodium* enzymes with the curated 48,544 drugs (Figure
370 1) and the possibility of repurposing them to target malaria.
371
372 We considered as candidates for targeting liver-stage malaria as the drugs or their metabolic
373 neighbors that show a good NICEdrug score (NICEdrug score above 0.5) with any of the 157
374 *Plasmodium* metabolite-enzyme pairs. We identified 516 such drug candidates, targeting 16
375 essential *Plasmodium* enzymes (Table S6, STAR Methods). Furthermore, 1,164 other drugs
376 appear in the metabolic neighborhood of the 516 identified drugs (between one and three
377 reaction steps away). Interestingly, out of the 516 identified drug candidates, digoxigenin,
378 estradiol-17beta and estriol have been previously validated as antimalarials (Antonova-Koch
379 et al., 2018) and NICEdrug.ch suggests their antimalarial activity relies on the competitive
380 inhibition of the KRC enzyme (Figure 6). This enzyme is part of both the steroid metabolism
381 and the fatty acid elongation metabolism, which we recently showed is essential for
382 *Plasmodium* liver-stage development (Stanway et al., 2019). Among the 516 NICEdrug
383 antimalarial candidates, there are also 89 molecules present in the metabolic neighborhood

384 of antimalarial drugs approved by (Antonova-Koch et al., 2018), which suggests these
385 antimalarials might be prodrugs (Table S6).
386
387 Being an intracellular parasite, antimalarial treatments should be efficient at targeting
388 *Plasmodium* as well as assure the integrity of the host cell (Figure 6A). To tackle this challenge,
389 we identified 1,497 metabolites participating in metabolic reactions catalyzed with essential
390 human enzymes (Table S5, STAR Methods) and excluded the antimalarial drug candidates that
391 shared reactive site-centric similarity with the extracted human metabolite set (to satisfy
392 NICEdrug score below 0.5). Out of all 516 drug candidates that might target liver-stage
393 *Plasmodium*, a reduced set of 64 molecules minimize the inhibition of essential human
394 enzymes (Table S6, STAR Methods) and are hence optimal antimalarial candidates.
395
396 Among our set of 64 optimal antimalarial candidates, a set of 14 drugs targeting the
397 *Plasmodium* shikimate metabolism, whose function is essential for liver-stage malaria
398 development (Stanway et al., 2019), arose as the top candidate because of its complete
399 absence in human cells. The set of drugs targeting shikimate metabolism include 40 prodrugs
400 (between one and three reaction steps away) that have been shown to have antimalarial
401 activity (Antonova-Koch et al., 2018) (Table S6). NICEdrug.ch identified molecules among the
402 prodrugs with a high number of toxic alerts, like nitrofen. It also identified four molecules
403 with scaffolds similar (two or three steps away) to the 1-(4-chlorobenzoyl)pyrazolidin-3-one
404 of shikimate and derivatives. This result suggests that downstream compounds of the 40
405 prodrugs might target the *Plasmodium* shikimate pathway, but also might cause side effects
406 in humans (Table S6).
407
408 To this end, NICEdrug.ch identified shikimate 3-phosphate as a top candidate antimalarial
409 drug. We propose that shikimate 3-phosphate inhibits the essential *Plasmodium* shikimate
410 biosynthesis pathway without side effects in the host cell (Figure 6, Table S6). Excitingly,
411 shikimate 3-phosphate has been used to treat *E. coli* and *Streptococcus* infections without
412 appreciable toxicity for patients (Díaz-Quiroz et al., 2018). Furthermore, recent studies have
413 shown that inhibiting the shikimate pathway using 7-deoxy-sedoheptulose is an attractive
414 antimicrobial and herbicidal strategy with no cytotoxic effects on mammalian cells (Brilisauer
415 et al., 2019). Experimental studies should now validate the capability of shikimate 3-

416 phosphate to efficiently and safely target liver malaria, and could further test other
417 NICEdrug.ch antimalarial candidates (Table S6).
418
419 ***NICEdrug.ch identifies over 1,300 molecules to fight COVID-19, with N-acetylcysteine as a***
420 ***top candidate***
421 SARS-CoV-2 is responsible for the currently on-going COVID-19 pandemic and the death of
422 around half a million people (as of today, June 15 (Dong et al., 2020)) and there is currently
423 no confirmed treatment for it. Attacking the host factors that allow replication and spread of
424 the virus is an attractive strategy to treat viral infections like COVID-19. A recent study has
425 identified 332 interactions between SARS-CoV-2 proteins and human proteins, which involve
426 332 hijacked human proteins or host factors (Gordon et al., 2020). Here, we first used
427 NICEdrug.ch to identify inhibitors of enzymatic host factors of SARS-CoV-2. Targeting such
428 human enzymes prevents interactions between human and viral proteins (PPI) (STAR
429 Methods, Figure 7A). Out of the 332 hijacked human proteins we identified 97 enzymes (STAR
430 Methods, Table S7) and evaluated their druggability by inhibitors among the 250,000 small
431 molecules in NICEdrug.ch and 80,000 molecules in food (STAR Methods, Figure 7A).
432 NICEdrug.ch suggests 22 hijacked human enzymes can be drug targets, and proposed 1301
433 potential competitive inhibitors from the NICEdrug.ch database. Out of 1301 potential
434 inhibitors, 465 are known drugs, 712 are active metabolic products of 1,419 one-step-away
435 prodrugs, and 402 are molecules in fooDB (Table S7). We found among the top anti SARS-
436 CoV-2 drug candidates the known reverse transcriptase inhibitor didanosine (Figure 7B, Table
437 S7), which other *in silico* screenings have also suggested as a potential treatment for COVID-
438 19 (Alakwaa, 2020; Cava et al., 2020). Among others, NICEdrug.ch also identified: (1)
439 actodigin, which belongs to the family of cardiotonic molecules proven to be effective against
440 MERS-CoV but without mechanistic knowledge (Ko et al., 2020), (2) three molecules in ginger
441 (6-paradol, 10-gingerol, and 6-shogaol) inhibiting catechol methyltransferase, and (3)
442 brivudine, a DNA polymerase inhibitor that has been used to treat herpes zoster (Wassilew,
443 2005) and prevent MERS-CoV infection (Park et al., 2019), and NICEdrug.ch suggests it for
444 repurposing (Figure S5, Table S7).
445
446 Drugs like remdesivir, EIDD-2801, favipiravir, and inhibitors of angiotensin converting enzyme
447 2 (ACE2) have been used to treat COVID-19 (Jeon et al., 2020), and act through a presumably

effective inhibitory mechanism (Figure S6A). For instance, the three drugs remdesivir, EIDD-2801, and favipiravir are believed to inhibit the DNA-directed RNA polymerase (E.C: 2.7.7.6). Here, we used the NICEdrug reactive site-centric fingerprint to seek for alternative small molecules in NICEdrug.ch and fooDB that could be repurposed to target ACE2 and DNA-directed RNA polymerase. NICEdrug.ch identified a total of 215 possible competitive inhibitors of ACE2. Among those is captopril, a known ACE2 inhibitor (Kim et al., 2003), and D-leucyl-N-(4-carbamimidoylbenzyl)-L-prolinamide, a NICEdrug.ch suggestion for drug repurposing to treat COVID-19. We also found 39 food-based molecules with indole-3-acetyl-proline (a molecule in soybean) as top ACE2 inhibitor candidate (Figure S6A, Table S8). To target the same enzyme as remdesivir, EIDD-2801, and favipiravir, NICEdrug.ch identified 1115 inhibitors of the DNA-directed RNA polymerase, like the drug vidarabine, which shows broad spectrum activity against DNA viruses in cell cultures and significant antiviral activity against infections like the herpes viruses, the vaccinia virus, and varicella zoster virus (Suzuki et al., 2006). We further found 556 molecules in food that might inhibit DNA-directed RNA polymerase, like trans-zeatin riboside triphosphate (FDB031217) (Table S8).

One of the host factors identified by Gordon and co-workers is the histone deacetylase 2 (HDAC2) (Gordon et al., 2020), which acetylates proteins and is an important transcriptional and epigenetic regulator. The acetyl and carboxylate moieties are the reactive sites of the forward (N6-acetyl-L-lysyl-[histone]) and reverse (acetate) biotransformation of HDAC2, respectively (Figure 7). NICEdrug.ch recognized a total of 640 drugs for repurposing that can inhibit HDAC2, including 311 drugs sharing the acetyl moiety and showing a NICEdrug score above 0.5 with respect to N6-acetyl-L-lysyl-[histone], and 329 drugs sharing the carboxylate moiety and presenting a NICEdrug score above 0.5 with acetate (STAR Methods). Among the drugs sharing the acetyl reactive site, we identified the known HDAC2 inhibitor melatonin (Wu et al., 2018), and to-our-knowledge new candidates like N-acetylhistamine and N-acetylcysteine. We also located 22 molecules in food with potential HDAC2 inhibitory activity, like N8-acetylspermidine (FDB022894) (Figure 7C, Table S8). Drugs sharing the carboxylate reactive site (as identified with NICEdrug) include the known HDAC2 inhibitors valproate, butyrate, phenyl butyrate (Abdel-Atty et al., 2014) and statins (Kong et al., 2004) (Figure 7C, Table S8). Interestingly, statins have been shown to have protective activity against SARS-CoV-2 (Lodigiani et al., 2020; Zhang et al., 2020). In addition and excitingly, the NICEdrug.ch

candidate N-acetylcysteine is a commonly used mucolytic drug that is sometimes considered as a dietary supplement and has putative antioxidant properties. Indeed, N-acetylcysteine is believed for long to be precursor of the cellular antioxidant glutathione (Mårtensson et al., 1989), but has unknown pharmacological action. NICEdrug.ch suggests that N-acetylcysteine might present a dual antiviral activity: firstly, N-acetylcysteine is converted to cysteine by HDAC2 and by that means, it is competitively inhibiting the native function of HDAC2 and interactions with viral proteins (Figure 7C, Table S8). Cysteine next fuels the glutathione biosynthesis pathway and produces glutathione in two steps.

Given the high coverage of validated molecules with activity against SARS-CoV-2 that NICEdrug.ch captured in this unbiased and reactive site-centric analysis, we suggest there might be other molecules in the set of 1,300 NICEdrug.ch candidates that could also fight COVID-19. Excitingly, there are many molecules that can be directly tested since these are drugs that have already passed all safety regulations or are molecules in food, like N-acetylcysteine for which we further reveal an action mechanism behind its potential anti SARS-CoV-2 activity. Other new candidates for which no safety data is available should be further validated experimentally and clinically. The mechanistic analyses provided by NICEdrug.ch could also guide new pharmacokinetic and pharmacodynamic models simulating SARS-CoV-2 infection and treatment.

Discussion

To systematically illuminate the metabolism and all enzymatic targets (competitively inhibited) of known drugs and hypothetical prodrugs to aid in the development of new therapeutic compounds, we used a proven reaction-prediction tool BNICE.ch (Hatzimanikatis et al., 2005) and an analysis of neighboring atoms of reactive sites analogous to BridgIT (Hadadi et al., 2019) and performed the first large-scale computational analysis of drug biochemistry and toxicity in the context of human metabolism. The analysis involved over 250,000 small molecules, and curation and computation of bio- and physicochemical drug properties that we assembled in an open-source drug database NICEdrug.ch that can generate detailed drug metabolic reports and can be easily accessed and used by researchers, clinicians, and industry partners. Excitingly, NICEdrug.ch revealed 20 million potential reactive sites at the 250,000 small molecules of the database, and there exist over 3,000

enzymes in the human metabolism that can be inhibited with the 250,000 molecules. This is because NICEdrug.ch can identify *all* potential metabolic intermediates of a drug and scans these molecules for substructures that can interact with catalytic sites across all enzymes in a desired cell.

NICEdrug.ch adapts the metric previously developed for reactions in BridgIT (Hadadi et al., 2019) to precisely compare drug-drug and drug-metabolite pairs based on similarity of reactive site and the neighborhood around this reactive site, which we have recently shown outperforms previously defined molecular comparison metrics (Hadadi et al., 2019). Since NICEdrug.ch shows high specificity in the identification of such reactive sites and neighborhood, it provides a better mechanistic understanding than currently available methods (Robertson, 2005). Despite these advances, it remains challenging to systematically identify non-competitive inhibition or targeting of non-enzymatic biological processes. We suggest coupling NICEdrug.ch drug metabolic reports with other *in silico* and experimental analyses accounting for signaling induction of small molecules and other non-enzymatic biological processes like transport of metabolites in a cell. The combined analysis of drug effects on different possible biological targets (not uniquely enzymes) will ultimately increase the coverage of molecules for which a mechanistic understanding of their mode of action is assigned.

A better understanding of the mechanisms of interactions and the specific nodes where the compounds act can help re-evaluate pharmacokinetic and pharmacodynamic models, dosage, and treatment. Such understanding can be used in the future to build models that correlate the pharmacodynamic information with specific compounds and chemical substructures in a manner similar to the one used for correlating compound structures with transcriptomic responses. We have shown for one of the most commonly used anticancer drugs, 5-FU, that NICEdrug.ch identifies and ranks alternative sources of toxicity and hence can guide the design of updated models and treatments to alleviate the drug's side-effects.

The mechanistic understanding will also further promote the development of drugs for repurposing. While current efforts in repurposing capitalize on the accepted status of known drugs, some of the issues with side effects and unknown interactions limit their development

544 as drugs for new diseases. Given that drug repurposing will require new dosage and
545 administration protocols, the understanding of their interactions with the human metabolism
546 will be very important in identifying, developing, and interpreting unanticipated side effects
547 and physiological responses. We evaluated the possibility of drug repurposing with
548 NICEdrug.ch as a substitute for statins, which are broadly used to reduce cholesterol but have
549 many side effects. NICEdrug.ch and its reactive site-centric comparison accurately cluster
550 both family types of statins, even though they are similar in overall molecular structure and
551 show different reactivity. In addition, NICEdrug.ch suggests a set of new molecules with
552 hypothetically less side effects (Endo and Hasumi, 1993; Tanaka et al., 2004) that share
553 reactive sites with statins.
554
555 A better mechanistic understanding of drug targets can guide the design of treatments
556 against infectious diseases, for which we need effective drugs that target pathogens without
557 side effects in the host cell. This is arguably the most challenging type of problem in drug
558 design, and indeed machine learning has continuously failed to guide such designs given the
559 difficulty in quantifying side effects—not to mention in acquiring large, consistent, and high-
560 quality data sets from human patients. To demonstrate the power of NICEdrug.ch for tackling
561 this problem, we sought to identify drugs that target liver-stage malaria parasites and
562 minimize the impact on the human host cell. We identified over 500 drugs that inhibit
563 essential *Plasmodium* enzymes in the liver stages and minimize the impact on the human host
564 cell. Our top drug candidate is shikimate 3-phosphate targeting the parasite's shikimate
565 metabolism, which we recently identified as essential in a high-throughput gene knockout
566 screening in *Plasmodium* (Stanway et al., 2019). Excitingly, our suggested antimalarial
567 candidate shikimate 3-phosphate has already been used for *Escherichia* and *Streptococcus*
568 infections without appreciable side effects (Díaz-Quiroz et al., 2018).
569 Finally, minimizing side effects becomes especially challenging in the treatment of viral
570 infections, since viruses fully rely on the host cell to replicate. As a last demonstration of the
571 potential of NICEdrug.ch, we sought to target COVID-19 by identifying inhibitors of 22 known
572 enzymatic host factors of SARS-CoV-2 (Gordon et al., 2020). NICEdrug.ch identified over 1,300
573 molecules that might target the 22 host factors and prevent SARS-CoV-2 replication. As a
574 validation, NICEdrug.ch correctly identified known inhibitors of those enzymes, and further
575 suggested safe drugs for repurposing and other food molecules with activity against SARS-

576 CoV-2. Among the NICEdrug.ch suggestions for COVID-19, based on the knowledge on its
577 mechanism and safety, we highlight N-acetylcysteine as an inhibitor of HDAC2 and SARS-CoV-
578 2.
579
580 Overall, we believe that a systems level or metabolic network analysis coupled with an
581 investigation of reactive sites will likely accelerate the discovery of new drugs and provide
582 additional understanding regarding metabolic fate, action mechanisms, and side effects and
583 can complement on-going experimental effects to understand drug metabolism (Javdan et
584 al., 2020). We suggest the generation of drug metabolic reports to understand the reactivity
585 of new small molecules, the possibility of drug repurposing, and the druggability of enzymes.
586 Our results using NICEdrug.ch suggest that this database can be a novel avenue towards the
587 systematic pre-screening and identification of drugs and antimicrobials. In addition to human
588 metabolic information, NICEdrug.ch currently includes information for the metabolism of *P.*
589 *berghei* and *E. coli*. Because we are making it publicly available (https://lcsb-
590 databases.epfl.ch/pathways/Nicedrug/), our hope is that scientists and medical practitioners
591 alike can make use of this unique database to better inform their research and clinical
592 decisions—saving time, money, and ultimately lives.
593

594 **Acknowledgements**

595 We would like to thank Dr. Ljubisa Miskovic, Dr. Volker T. Heussler, Dr. Reto Caldelari, Dr. Jens
596 Nielsen, and Dr. Adil Mardinoglu for critical feedback and discussions. The graphical abstract
597 and Figures 6, 7, S5, and S6 were done with BioRender. H.M. was funded by the European
598 Union's Horizon 2020 research and innovation program under the Marie Skłodowska-Curie
599 grant agreement No 72228. H.M., K.H. and J.H. were supported by the Ecole Polytechnique
600 Fédérale de Lausanne (EPFL). A.C. and V.H. were funded by grant 2013/155 (MalarX), N.H.
601 and J.H. were funded by grant 2013/158 (MicroScapesX); both are SystemsX.ch grants
602 awarded by the SNSF.
603

604 **Author Contributions**

605 Conceptualization, V.H., H.M., N.H., A.C-P.; Methodology, V.H., H.M., K.H., N.H., A.C-P.;
606 Software, H.M., K.H., J.H.; Formal analysis, H.M., K.H.; Investigation, H.M., K.H., A.C-P.;
607 Writing- Original Draft, H.M., A.C-P.; Writing- Review & Editing, V.H., H.M., A.C-P., J.H., N.H.;

Visualization, H.M., A.C-P.; Supervision, V.H.; Project Administration, V.H., H.M.; Funding Acquisition, V.H.

Declaration of interests

The authors declare no competing interests.

Main figure title and legends

Figure 1. Pipeline to construct and use the NICEdrug.ch database.

NICEdrug.ch (1) curates available information and calculates the properties of an input compound; (2) identifies the reactive sites of that compound; (3) explores the hypothetical metabolism of the compound in a cell; (4) stores all functional, reactive, bio-, and physico-chemical properties in open-source database; and (5) allows generation of reports to evaluate (5a) reactivity of a small molecule, (5b) drug repurposing, and (5c) druggability of an enzymatic target. See also Figure S1, Figure S2, Figure S3, and Table S1.

Figure 2. Similarity in reactive site and neighborhood defines para-metabolites in 5-FU metabolism and inhibited human metabolic enzymes.

Eight para-metabolites in the 5-FU metabolic neighborhood (represented as defined in Materials and Methods). We show the most similar native human metabolites, inhibited enzymes, and native products of the reactions. See also Table S2.

Figure 3. A different reactive site but similar neighborhood defines top anti-metabolites in 5-FU metabolism and inhibited human metabolic enzyme.

Eight anti-metabolites of dUMP in the 5-FU metabolic neighborhood (represented as defined in Materials and Methods). Note that the reactive site of the anti-metabolites is different than the one of the native human metabolite, but the neighborhood is highly similar, which determines the high NICEdrug score (value in parenthesis). We show the inhibited human enzyme (dTMP synthase) and reaction, and its native product. See also Table S2.

Figure 4. Comparing downstream products to known toxic molecules and analyzing their common structural toxic alerts explains metabolic toxicity of 5-FU.

639 Example of six suggested toxic molecules in the 5-FU metabolic neighborhood (represented
640 as defined in Materials and Methods). We show toxic compounds from the supertoxic and
641 hepatotoxic databases that lead to the highest NICEdrug toxicity score (number under toxic
642 intermediate name, Materials and Methods). We highlight functional groups linked to five
643 NICEdrug toxic alerts (legend bottom right). See also Table S2.
644
645 **Figure 5. Clustering of molecules with statin reactive sites based on NICEdrug score suggests**
646 **drugs for repurposing.**
647 **(A)** Pairwise NICEdrug score between all molecules with statin reactive sites (heat map) and
648 number of metabolic reactions in which they participate (right). We highlight clusters of
649 statins of type 1 (cluster a) and type 2 (cluster b), and clusters of most similar molecules to
650 type 1 statins (cluster c) and type 2 statins (cluster d). Within the metabolic reactions, we
651 indicate the total number of reactions (dark color) and the number of reactions that involve
652 the statin reactive site (light color). **(B)** Examples of statins and Mevastatin analogues of type
653 1 from cluster c (blue) and of type 2 from cluster d (gold). We left the known statins
654 unmarked, which are appropriately clustered together based on the NICEdrug score, and we
655 mark with * new molecules that cluster with statins and that NICEdrug.ch suggests could be
656 repurposed to act as statins. Reactive sites in type 1 statins and type 2 statins are colored in
657 blue and orange, respectively. The reactive site neighborhood as considered in the NICEdrug
658 score is also marked. See also Figure S3, Figure S4, Table S3, and Table S4.
659
660 **Figure 6. NICEdrug.ch suggests shikimate 3-phosphate as a top candidate to target liver-**
661 **stage malaria and minimize side effects in host human cells.**
662 **(A)** Schema of ideal scenario to target malaria, wherein a drug efficiently inhibits an essential
663 enzyme for malaria parasite survival and does not inhibit essential enzymes in the host human
664 cell to prevent side effects. **(B)** Shikimate 3-phosphate inhibits enzymes in the *Plasmodium*
665 shikimate metabolism, which is essential for liver-stage development of the parasite.
666 Shikimate 3-phosphate does not inhibit any enzyme in the human host cell since it is not a
667 native human metabolite, and it does not show similarity to any native human metabolite.
668 **(C)** Mechanistic details of inhibition of aroC by shikimate 3-phosphate and other NICEdrug
669 candidates. See also Table S5 and Table S6.
670

671 **Figure 7. NICEdrug strategy to fight COVID-19, and NICEdrug candidate inhibitors of SARS-**
672 **CoV-2 host factors: reverse transcriptase and HDAC2.**
673 **(A)** Schema of NICEdrug strategy to target COVID-19, wherein a drug (top-left) or molecules
674 in food (top-right) efficiently inhibit a human enzyme hijacked by SARS-CoV-2. Inhibition of
675 this host factor reduces or abolishes protein-protein interactions (PPI) with a viral protein and
676 prevents SARS-CoV-2 proliferation. **(B)** Inhibition of the reverse transcriptase (E.C: 1.1.1.205
677 or P12268) and the PPI with SARS-CoV-nsp14 by didanosine based on NICEdrug.ch. **(C)**
678 Inhibition of the HDAC2 (E.C: 3.5.1.98) and the PPI with SARS-CoV-nsp5 by molecules
679 containing acetyl moiety (like melatonin, N-acetylcysteine, and N8-acetylspermidine), and
680 molecules containing carboxylate moiety (like valproate, stains, and butyrate) based on
681 NICEdrug.ch. See also Figure S5, Figure S6, Table S7, and Table S8.
682
683 **Supplementary figure title and legends**
684 **Supplementary figure 1. Overview of number of molecules in NICEdrug.ch and their**
685 **structural curation, related to Figure 1.**
686 **(A)** Venn diagram showing the number of compounds in NICEdrug.ch and their source
687 database: KEGG, DrugBank, ChEMBLE NTD, and ChEMBLE. **(B)** Representation on how
688 different kekulé forms affect the identification of reactive sites and prediction of biological
689 activity for an example molecule.
690
691 **Supplementary figure 2. Distribution of reactive sites and metabolic reactions as of E.C.**
692 **numbers linked to all molecules in NICEdrug.ch, related to Figure 1.**
693 **(A)** Distribution of reactive sites identified in all molecules of NICEdrug.ch among classes of
694 E.C. numbers. **(B)** Specificity of reactive sites identified in drugs based on length and types of
695 participating atoms. **(C)** Distribution of drug metabolic reactions based on class of E.C.
696 number. **(D)** Distribution of Gibbs free energy for the drug metabolic reactions, which are the
697 reactions linked to all molecules of NICEdrug.ch.
698
699 **Supplementary figure 3. Description of NICEdrug score, related to Figures 1, 2, 3, 4, 5, and**
700 **6.**

701 Example of NICEdrug score calculation. The NICEdrug score takes into account the structure
702 of a molecule's reactive site and its seven-atom-away neighborhood for similarity evaluation,
703 analogous to BridgIT.
704
705 **Supplementary figure 4. Clustering based on NICEdrug score, molecular weight, and**
706 **reactivity of statin like molecules, related to Figure 5.**
707 Hierarchical clustering based on the NICEdrug score of all molecules in NICEdrug.ch that
708 contain statin reactive site (left). We report the molecules' molecular weight (middle left) and
709 number of drug metabolic reactions or reactions in which these drugs participate (middle).
710 The molecular weight seems to be inversely correlated with the number of drug metabolic
711 reactions. We highlight six clusters of drugs (a-f, middle right) and an example representative
712 molecule (left). Interestingly, these clusters also group molecules based on bio- or physico-
713 chemical properties: "cluster a" involves a range of silicon-containing chemical molecules,
714 "cluster b" are drug like molecules of type 2 statins, "cluster c" includes chemical molecules
715 with a long chain connected to the reactive site, "cluster d" involves molecules with 1-
716 indanone fused with a tetrahydropyran ring, "cluster e" comprises drug-like molecules of type
717 1 statins, and "cluster f" are 16-membered ring macrolide antibiotics.
718
719 **Supplementary figure 5. NICEdrug candidate inhibitors of SARS-CoV-2 host factors:**
720 **galactosidase, catechol methyltransferase, and DNA polymerase, related to Figure 7.**
721 **(A)** Inhibition of the galactosidase (E.C: 3.2.1.22 or P06280) and the PPI with SARS-CoV-2
722 nsp14 by actodigin based on NICEdrug.ch. **(B)** Inhibition of the catechol methyltransferase
723 (E.C: 2.1.1.6 or P21964) and the PPI with SARS-CoV-2 nsp7 by 6-paradol, 10-gingerol, and 6-
724 shogaol, which are molecules in ginger, based on NICEdrug.ch. **(C)** Inhibition of the DNA
725 polymerase (E.C: 2.4.1.-) and the PPI with SARS-CoV-2 nsp8 by brivudine based on
726 NICEdrug.ch.
727
728 **Supplementary figure 6. NICEdrug candidate inhibitors of ACE2, related to Figure 7.**
729 Inhibition of the ACE2 (E.C: 3.4.17.23), a putative host factor of SARS-CoV-2, by the known
730 inhibitor captopril, and NICEdrug candidates D-leucyl-N-(4-carbamimidoylbezyl)-L-
731 prolinamide and indole-3-acetyl-proline.
732

Materials and Methods

Representation of metabolic neighborhood in figures of this manuscript

We represent the metabolic neighborhood of a drug with reactions or steps away (arrows), where each step away (circle connected to arrow) involves a set of compounds. We extract compounds at each step that present a high NICEdrug score (value under metabolite name) with the native substrate of a reaction in the human cell. Reactive sites common to neighbor metabolites and native human metabolites are shaded with colors matching the color of the enzymes (packmen) that are inhibited. The neighborhood (seven atoms away, as considered in NICEdrug score) of the reactive sites is circled in the metabolites and native human metabolites with the same color as the reactive sites and enzymes. Compounds marked with * are confirmed inhibitors and references are provided in the main text.

Representation of enzymatic inhibition in figures of this manuscript

We represent the enzymes and catalyzed reactions inhibited by NICEdrug candidates. Highlighted are the reactive site and neighborhood (as considered in the NICEdrug score) in candidate drugs and metabolites, which are native substrates of the human enzymes. The SARS-CoV-2 proteins interaction with the enzyme is presumed to be diminished or abolished upon inhibition of the human enzyme. Compounds marked with * are confirmed inhibitors and references are provided in the main text.

Curation of input molecules used in the construction of NICEdrug.ch

We constructed the NICEdrug.ch database to gather small molecules suitable for treatment of human diseases. We collected the SMILES structure, synonyms, and any available bio- and physico-chemical property included from three source databases: KEGG, ChEMBL, and DrugBank, which added up to 70,976 molecules by January 2018 (Figure S1A). Only molecules that were fully structured were imported to our database. We further curated the imported molecules by removing duplicate structures and merging annotations from different databases into one molecule entry in the database. For removing duplicate structures we used canonical SMIELS (Weininger, 1988) generated by openbabel (O'Boyle et al., 2011) version 2.4.0. This unification method is based on atoms and their connectivity in a molecule in terms of a molecular graph that is captured by the canonical SMILES. Therefore, different resonance forms, stereoisomers, as well as dissociated and charged states of the same

765 compound are mapped to one entry in database. Furthermore, we filtered molecules based
766 on Lipinski rules (Lipinski et al., 2001): (1) the molecular weight should be less than 500
767 Dalton, (2) the number of hydrogen bond donors should be less than five, (3) the number of
768 hydrogen bond acceptors should be less than ten, and (4) an octanol-water partition
769 coefficient (log P) should be less than five. According to Lipinski rules an active orally drug
770 does not violate more than one of the above criteria. We calculated criteria one, two and
771 three based on the structural information from SMILES of molecules. To assess criterion four,
772 we relied on reported data in the source database. We kept in the NICEdrug.ch database
773 those compounds for which the partition coefficient was not available.
774 We performed a separate analysis to account for non-unique graph representations of
775 aromatic rings, also called *kekulé structures*. The existence of aromatic rings and the fact that
776 bond-electrons are shared within the ring make several single-double bond assignments
777 possible, which results in multiple kekulé representations for a single molecule (Figure S1B).
778 We included all such kekulé structures to account for alternative atom-bond connectivity and
779 associated reactivity. We call "effective forms" to the kekulé representations that show
780 different reactive sites than their canonical structures. For example, there can be two
781 effective forms plus the canonical structure (Figure S1B). In total, we found 42,092 effective
782 forms for 29,994 aromatic compounds in NICEdrug.ch database and we kept them for further
783 analysis.
784 We also computed the thermodynamic properties of all drugs in NICEdruch.ch. Specifically,
785 we computed the Gibbs free energy of formation ($\Delta_f G'^{\circ}$) using the group contribution method
786 of Mavrovouniotis (Jankowski et al., 2008).
787 The NICEdrug.ch database includes a total number of 48,544 unique and curated small
788 molecules (Figure S1A).
789

790 **Identification of reactive sites in drugs**

791 The 3D structures of enzyme pockets are complex and mostly unknown. Therefore, evaluating
792 and comparing docking of two small molecules in the pocket of a specific target is impossible
793 most of the times. Using BNICE.ch, we focused on the complementary structure of active sites
794 on substrates, also called *reactive site*. To recognize the potential reactive sites on molecules,
795 we scanned molecules using expert-curated generalized reaction rules of BNCIE.ch (Hadadi et
796 al., 2016), which mimic the identification of substrates by the enzyme pocket and account for

797 the promiscuous activity of enzymes. Theses reaction rules incorporate the information of
798 biochemical reactions and have third-level Enzyme Commission (EC) identifiers. Each
799 BNICE.ch reaction rule accounts for three levels of information: (1) atoms in reactive sites of
800 compounds, (2) connectivity and configuration of atom bonds in the reactive site, and (3)
801 mechanism of bond breakage and formation during the reaction. As of May 2020, BNICE.ch
802 contains 450 bidirectional generalized reaction rules that can reconstruct 8118 KEGG
803 reactions (Hadadi et al., 2016). Here, we include all BNICE.ch rules to identify all possible
804 reactive sites on a given drug in two steps. First, a BNICE.ch rule identifies all atoms in a
805 compound that belong to the rule's reactive site. Second, the rule evaluates the connectivity
806 of the atoms previously identified. The candidate compounds for which a BNICE.ch rule
807 identified a reactive site were validated as metabolically reactive and considered for analysis
808 in NICEdrug.ch.
809 It is important to note that thanks to the generalized reaction rules, which abstract the
810 knowledge of thousands of biochemical reactions, BNICE.ch is able to reconstruct known
811 biotransformations and also propose novel metabolic reactions. This was demonstrated in
812 the reconstruction of the ATLAS of Biochemistry (Hadadi et al., 2016), which involves up to
813 130,000 reactions between known compounds.
814
815 **Analysis of drug metabolism in human cells.**
816 To mimic biochemistry of human cells and simulate human drug metabolism, we collected all
817 available information (metabolites and metabolic activities or EC numbers of enzymes) on
818 human metabolism from three available databases: the human metabolic models Recon3D
819 (Brunk et al., 2018) and HMR (Pornputtapong et al., 2015), and the Reactome database (Croft
820 et al., 2011). These three databases include a total of 2,266 unique human metabolites and
821 2,066 unique EC numbers of enzymes (Table S1).
822 To explore the biochemical space beyond the known human metabolic reactions and
823 compounds, we used (1) the generalized enzymatic reaction rules of BNICE.ch that match up
824 to the third EC level the collected human enzymes, and (2) all of the collected human
825 metabolome. We evaluated the reactivity of each drug in a human cell using the retro-
826 biosynthesis algorithm of BNICE.ch, which predicts hypothetical biochemical transformations
827 or *metabolic neighborhood* around the drug of study. We generated with BNICE.ch metabolic
828 reactions in which each drug and all known human metabolites could participate as substrate

829 or products. We also allowed a set of 53 known cofactors to react with the human
830 metabolites (Table S1).
831 We define the boundaries of the metabolic neighborhood of a molecule with a maximum
832 number of reactions or *steps away* that separate the input molecule (drug of study) from the
833 furthest compound. In BNICE.ch, a generation *n* of compounds involves all metabolites that
834 appear for the first time in the metabolic neighborhood of a drug after *n* reactions or steps
835 happened. For example, in the case study of 5-FU we find the compound 5-Fluorouridine in
836 generation 2 or 2 steps away, which means there are two metabolic reactions that separate
837 5-FU and 5-Fluorouridine (Figure 2).
838 In NICEdrug.ch, there exist 197,246 compounds in generation 1 (1 step away) from all input
839 drugs. The 197,246 compounds are part of the potential drug metabolic neighborhood in
840 human cells. Out of all generation 1 molecules, 13,408 metabolites can be found in human
841 metabolic models and HMDB database (Wishart et al., 2018), 16,563 metabolites exist in
842 other biological databases, and the remaining 167,245 metabolites are catalogued as known
843 compounds in chemical databases (i.e., PubChem). Note that HMDB includes native human
844 metabolites and non-native human compounds, like food ingredients.
845 The 197,246 products that are one-step away of all NICEdrug.ch molecules are part of a
846 hypothetical biochemical neighborhood of 630,449 drug metabolic reactions. Of all drug
847 metabolic reactions, 5,306 reactions are cataloged in biological databases, and the remaining
848 625,143 reactions are novel. A majority of the reactions involved oxidoreductases (42.54%),
849 broken down into 27.45% of lyases, 7.15% of hydrolases, 6.28% of transferases, 1% of
850 isomerases, and 15.58% of ligases. Interestingly based on the previously identified reactive
851 sites, out of the 265,935 (42.54% of 625,143) oxidoreductase reactions, 49.92% are catalyzed
852 by the p450 family of enzymes, which are known to be responsible for the metabolism of drug
853 (Figure S2C).
854

855 **Using NICEdrug.ch database for analysis of the metabolic neighborhood of a drug**

856 In NICEdrug.ch webserver, users can look up for a drug using the drugs' name and other
857 identifiers like ChEMBL, DrugBank and KEGG. NICEdrug.ch will report a unique identifier for
858 the compound that will be input for upcoming analysis modules. The *predict metabolism*
859 module allows to study the metabolic network around an input molecule. The input to this
860 module is: (1) the unique identifier of the drug of interest, (2) a maximum number of reactions

or *steps away* that shall separate the input drug to the furthest compound in the metabolic neighborhood.

The output of this analysis is a report in the form of a csv file that includes all compounds and metabolic reactions in the metabolic neighborhood of the input drug. One can also export the neighborhood in the form of a visual graph, in which nodes are molecules and edges are reactions.

Definition of the NICEdrug score

Based on the theory of lock and key, two metabolites that can be catalyzed by the same enzyme may have similar reactive sites and also neighboring atoms. In order to quantify the similarity inside and around reactive sites of <u>two molecules</u>, we developed a metric called *NICEdrug score* (Figure S3), which is inspired on BridgIT (Hadadi et al., 2019). BridgIT assesses the similarity of <u>two reactions</u>, considering the reactive site of the participating substrates and their surrounding structure until the seventh atom out of the reactive site.

The NICEdrug score is an average of two similarity evaluations: (1) the atom-bond configuration inside reactive site (α parameter), and (2) the 7 atom-bond chain molecular structure around the reactive site (β parameter). The NICEdrug score, and its parameters α and β, range between 0 and 1 when they indicate no similarity and identical structure, respectively. Different constraints on the α and β parameters determine the identification of different types of inhibition like para-metabolites and anti-metabolites (see other sections in this Materials and Methods).

We show the evaluation of NICEdrug scores for three example compounds (Figure S3). In this example, Digoxin, Labriformidin and Lanatoside C all share the reactive site corresponding to EC number 5.3.3.- (α=1). Starting from the atoms of the identified reactive site, eight description layers of the molecule were formed, where each layer contains a set of connected atom-bond chains. Layer zero includes types of atoms of reactive site and their count. Layer 1 expands one bond away from all of the atoms of reactive site and accounts for atom-bond-atom connections. This procedure is continued until layer 7, which includes the sequence of 8 atoms connected by 7 bonds. Then, we compare the fingerprint of each molecule to the other participants of the class based on the Tanimoto similarity scores. A Tanimoto score near 0 designates no or low similarity, whereas a score near 1 designates high similarity in and

around reactive site. Lanatoside C and Digoxin share the same substructure till 8 layers out of reactive site which is presented in the NICEdrug score by preserving score 1 in all layers, so the overall Tanimoto score for these two compounds in the context of EC number 5.3.3.- is 1 (α=1 and β=1). However, the structure of two compounds are not exactly the same and actually Lanatoside C has 8 more carbon atoms and 6 more oxygen atoms, shaped as an extra benzenehexol ring and an ester group. Although this part is far from the reactive site, based on the NICEdrug score they both can perfectly fit inside the binding pocket of a common protein related to this reactive site. This hypothesis is proved by experiments reported in KEGG and DrugBank. According to DrugBank and KEGG, Lanatoside C has actions similar to Dioxin and both of them have the same target pathways: Cardiac muscle contraction and Adrenergic signaling in cardiomyocytes. Furthermore, target protein for both of them is ATP1A.

Also, the NICEdrug score effectively captures and quantifies differences around the reactive site. The substructure around the reactive site in Labriformidin is slightly different (α=1 and β <1). The difference is calculated trough different layers of the NICEdrug score.

In the case study of 5-FU, in order to predict competitive inhibition, we analyzed all the metabolites that share reactive site with 5-FU or its downstream products (α=1) and then we ranked the most similar metabolites based on their similarity in neighborhood of reactive site to 5-FU or its downstream products (β). To assess the structural differences in the reactive sites themselves (α), we implemented the Levenshtein edit distance algorithm (Levenshtein, 1966) to determine how many deletions, insertions, or substitutions of atom/bonds are required to transform one pattern of reactive site into the other one. Here, the edit distance explains the difference between the reactive sites of the intermediate and the human metabolite. However, even slight changes in the reactive site affect its interaction with the binding site. To ensure that the divergence retained the appropriate topology, we compared the required edit on reactive site with interchangeable groups, termed bioisosteric groups (Papadatos and Brown, 2013). These bioisosteric groups contain similar physical or chemical properties to the original group and largely maintain the biological activity of the original molecule. An example of this is the replacement of a hydrogen atom with fluorine, which is a similar size that does not affect the overall topology of the molecule. For this analysis, we

922 used 12 bioisosteric groups adapted from the study by Papadatos et.al. (Papadatos and
923 Brown, 2013).
924 To predict irreversible Inhibitors in metabolism of 5-FU, we kept only molecules with a
925 similarity score greater than 0.9 to metabolites (β>0.9), to preserve a high similarity in the
926 neighborhood of the reactive sites. Then, we checked which ones contained reactive sites
927 that differed only in the replacement of bioisosteric groups (α~1).
928

929 **Classification of drugs based on the NICEdrug score**

930 Classification of compounds with similar structure is normally used to assign unknown
931 properties to new compounds. For instance, one can infer ligand-protein binding for a drug
932 when its action mechanism or the structure of the target proteins are not known. In this study,
933 we have demonstrated four strategies to classify drugs (Figure 1), which are from less to more
934 stringent: classifying (1) molecules that participate in reactions with the same EC up to the 3th
935 level, (2) molecules that in addition share a BNICE.ch reaction rule, (3) molecules that in
936 addition to both previous points share reactive site, (4) molecules that show high similarity of
937 reactive site and neighborhood based on the NICEdrug score.
938 The EC number guarantees that molecules are catalyzed with similar overall reaction
939 mechanism. Generalized reaction rules from BNICE.ch further capture different
940 submechanisms inside an EC number (Hadadi et al., 2016). A BNICE.ch reaction rule might
941 involve more than one reactive site. Hence, information of reactive sites provide further
942 insights into the molecule's reactivity. Furthermore, similarity of reactive sites and their
943 neighborhoods based on the NICEdrug score increase the comparison resolution and this is
944 the basis of the classification in NICEdrug.ch.
945 In NICEdrug.ch database there exist 95,342 classes that comprise all drugs and human
946 compounds sharing EC, BNICE.ch rule, and reactive site (classification based on our strategy
947 3). We computed the NICEdrug score between all pairs of molecules in a class and this
948 information is available in NICEdrug.ch.
949

950 **Identification of drugs acting as para-metabolites based on NICEdrug score**

951 Small molecules that share reactive site and are structurally similar to native human
952 metabolites enter and bind the pocket of native enzymes and competitively inhibiting

953 catalysis acting as para-metabolites (Ariens, 2012). In this study, we define as para-metabolite
954 any drug or any of its metabolic neighbors that (1) shares reactive site with native metabolites
955 (α=1), and (2) preserves a high NICEdrug score with respect to the reactive site neighborhood
956 (β>0.9).
957

958 **Identification of drugs acting as anti-metabolites based on NICEdrug score**

959 Small molecules that do not share reactive site but are structurally similar to native human
960 metabolites might enter the binding pocket of native enzymes and inhibiting catalysis acting
961 as anti-metabolites (Ariens, 2012). In this study, we define as anti-metabolite any drug or any
962 of its metabolic neighbors that (1) differs slightly in reactive site from a native metabolite
963 (α~1), and (2) preserves high similarity in the reactive site neighborhood (β>0.9). We
964 hypothesize that a low divergence in the reactive site, still allows a non-native compound to
965 enter and bind the enzyme pocket since it is structurally similar enough to the native
966 substrate.
967

968 **Identification of NICEdrug toxic alerts**

969 We obtained all NICEdrug toxic alters from ToxAlert database (Sushko et al., 2012). ToxAlert
970 database includes about 1,200 structural toxic alerts associated with particular types of
971 toxicity. Toxic alerts are provided in the form of SMART patterns that are searchable in SMILES
972 structure of molecules. NICEdrug.ch uses openbable tool (O'Boyle et al., 2011) to search for
973 these structural alerts on SMILES of compounds.
974

975 **Collection of reference toxic molecules in NICEdrug.ch**

976 Studying the adverse effects of chemicals on biological systems has led to development of
977 databases cataloging toxic molecules. The Liver Toxicity Knowledge Base (LTKB) integrates
978 1,036 molecules annotated with human Drug-induced liver injury risk (severity). Super toxic
979 DB include about 60k toxic molecules, that are annotated with their toxicity estimate,
980 LC_{50}/LD_{50} i.e., lethal dose or concentration at which 50% of a population dies.
981 As a resource of approved toxic molecules, we collected all of the molecules cataloged as
982 toxic in LTKB and super toxic databases. We used this collection as a reference to compare
983 the similarity of drugs or and products of drug metabolism with approved toxic molecules.

984

985 **Definition of a toxicity score in NICEdrug.ch**

986 The number of molecules labeled as toxic in databases is disproportionally low compared to
987 the space of compounds. On the other hand, toxic alerts are defined for a big number of
988 compounds and are linked to redundant molecular structures.

989 We measured the similarity of drugs and their metabolic neighbors with the collection of
990 reference toxic molecules using the NICEdrug score. We assigned toxic alerts to molecules in
991 NICEdrug.ch if a molecule and toxic molecule shared a molecular substructure linked to the
992 toxic alert.

993 Finally, NICEdrug.ch provides a toxicity report in the form of a csv file for each molecule in the
994 metabolic neighborhood including six values linked to the most similar toxic molecules in both
995 toxic reference databases (LTKB and supertoxic databases): (1) the NICEdrug score between
996 the drug and those most similar toxic molecules, (2) the severity degree of the hepatotoxic
997 compound, and log(LC_{50}) of the supertoxic compound, and (3) the number of common toxic
998 alerts between the drug and the most similar toxic molecules. The list of toxic alerts is also
999 provided.

1000 We combined the six values of the toxicity report into a toxicity score defined as follows:

1001

1002 $$\sum_{i} \text{NICEdrug score} \times (\log(\text{LC}_{50}) \text{ or severity degree})$$

1003 $$\times \text{ number of common NICEdrug toxic alerts}$$

1004 $$\text{i} \in \{\text{the most similar approved toxic molecules in LTKB and supertoxic databases}\}$$

1005

1006 The toxicity score in NICEdrug.ch served to quantify the toxicity of each molecule in the
1007 metabolic neighborhood of a drug, recapitulate known toxic molecules, and suggest new toxic
1008 compounds (Figure 4).

1009

1010

1011 **Analysis of essential enzymes and linked metabolites in *Plasmodium* and human cells**

1012 We extracted information of essential genes and enzymes for liver-stage malaria
1013 development from our recent study (Stanway et al., 2019). In this study, we developed the
1014 genome-scale metabolic model of *Plasmodium berghei*, which shows high consistency

1015 (approximately 80%) with the largest gene knockout datasets in *Plasmodium* blood (Bushell
1016 et al., 2017) and liver stages (Stanway et al., 2019). There are 178 essential genes for *P.*
1017 *berghei*'s growth simulating liver-stage conditions (Stanway et al., 2019). Here, we identified
1018 the substrates of those essential metabolic enzymes, which comprise a set of 328 metabolites
1019 (Table S5). To further minimize on the host cell, we filtered out those *Plasmodium* enzymes
1020 that share 4th level E.C. with human essential enzymes. We used available CRISPR gene
1021 essentiality data in various human cell lines (Wang et al., 2015) to identify essential genes and
1022 enzymes in human cells (Table S5). We further identified essential metabolites in human cells
1023 (Table S5) using the latest human genome-scale metabolic model (Robinson et al., 2020) and
1024 the metabolic information associated to the essential human genes. Subtracting essential
1025 parasite and human enzymes resulted in the analysis of 32 essential *Plasmodium* enzymes
1026 catalyzing 68 metabolites and 157 unique metabolite-enzyme pairs in the parasite (Table S6).
1027

1028 **Identification of drugs to target malaria and minimize side effects on human cells**

1029 Those molecules that themselves and their downstream products cannot act as inhibitors of
1030 essential metabolic enzymes in the human host cell while they can target essential
1031 *Plasmodium* enzymes are attractive antimalarial candidates.

1032 We first used NICEdrug.ch to look for small molecules that share reactive site with the 32
1033 essential *Plasmodium* enzymes and they have good similarity score in reactive site
1034 neighborhood to native substrates of essential enzymes of parasite, i.e. NICEdrug score above
1035 0.5 (Table S6). We also identified prodrugs that might lead to downstream products with
1036 similar reactive site and neighborhood (NICEdrug above 0.5) to any of the essential
1037 *Plasmodium* metabolites (Table S6). We suggest those drugs and downstream products act
1038 as antimetabolites and competitively inhibit the essential enzymes in the parasite. Overall,
1039 we identified 516 drugs that directly compete with essential metabolites and 1,164 prodrugs
1040 that need to be biochemically modified between one to three times in human cell to render
1041 inhibition of essential enzymes.

1042 We next combined information of essential *Plasmodium* and human metabolites to screen
1043 further the drug search using NICEdrug.ch. Out of the hypothetical 516 antimalarial
1044 candidates, we identified 64 drugs that share reactive site with parasite metabolites
1045 (NICEdrug score above 0.5) and not with human metabolites (NICEdrug score below 0.5),
1046 making them good candidates for drug design (Table S6).

1047

1048 **Prediction of inhibitors among food based molecules**

1049 We used the reactive site-centric fingerprint available in NICEdrug.ch to identify molecules in
1050 food that share reactive site with native substrates of human enzymes and hence might
1051 inhibit those enzymes. We retrieved the total set of 80,000 compounds from FooDB (Scalbert
1052 et al., 2011), and treated them as input molecules into the NICEdrug pipeline (Figure 1) to
1053 identify reactive sites and evaluate their biochemistry, as done for all molecules in
1054 NICEdrug.ch.

1055

1056 **Identification of small molecules to target COVID-19**

1057 A recent study reported 332 host factors of SARS-CoV-2 (Gordon et al., 2020). Out of the 332
1058 proteins, 97 have catalytic function and EC number assigned, and are potential targets of
1059 small molecules. We evaluated the druggability of these 97 enzymes using NICEdrug.ch.
1060 To generate a druggability report, NICEdrug.ch first gathers the metabolic reactions
1061 associated with the protein EC numbers. NICEdrug.ch uses 11 databases (including HMR,
1062 MetaCyc, KEGG, MetaNetX, Reactome, Rhea, Model SEED, BKMS, BiGG models and Brenda)
1063 as source of metabolic reactions. All these databases involve a total of 60k unique metabolic
1064 reactions.
1065 Out of the 97 host factor enzymes, we identified 22 enzymes that are linked to fully-defined
1066 metabolic reactions. Fully-defined metabolic reactions fulfill three criteria. (1) There is a
1067 secondary structure available for all the reaction participants, which means there are
1068 available mol files. (2) There is a fully defined molecular structure for all the reaction
1069 participants, which means molecules with unspecified R chains are discarded. (3) There is a
1070 BNICE.ch enzymatic reaction rule assigned to the reaction (Table S7).
1071 NICEdrug.ch identified 22 host factor enzymes with 24 unique linked EC numbers and 145
1072 unique fully defined reactions. NICEdrug.ch extracts the metabolites participating in these
1073 reactions and identifies their reactive site for a reactive-site centric similarity evaluation
1074 against a list of molecules. To this end, NICEdrug.ch reports the list of molecules ranked based
1075 on the NICEdrug score. The molecule with the highest NICEdrug score shares the highest
1076 reactive site-centric similarity with the native substrate of the target enzyme (Table S7).
1077 We found 1,301 molecules that show NICEdrug score above 0.5 with respect to substrates of
1078 the 22 SARS-CoV-2 hijacked enzymes (Table S7). Out of 1,301 molecules, 465 are drugs

1079 cataloged in DrugBank, KEGG drugs or ChEMBL databases, 712 are active molecules one step
1080 away of 1,419 prodrugs, and 402 are food molecules (Table S7).
1081 To better understand the classes of drugs or food molecules, we classified drugs based on
1082 their KEGG drug groups (Dgroups) and food molecules based on their food source. Out of 465
1083 drugs identified, 43 drugs are assigned to 55 different Dgroups and 402 food molecules belong
1084 to 74 different food sources (Table S7).
1085

1086 **Supplemental table titles and legends**

1087 **Table S1. Information of human metabolism considered in this study, related to Figures 2,**
1088 **3, 4, 5, and 6.**
1089 **(A)** List of cofactors, **(B)** list of metabolites, and **(C)** list of E.C. numbers considered in BNICE.ch
1090 for the generation of reactions in the analysis of drug metabolism in a human cell (Materials
1091 and Methods).
1092

1093 **Table S2. Metabolic neighborhood of 5-FU, related to Figures 2, 3, and 4.**
1094 **(1)** List of compounds in the 5-FU metabolic neighborhood including up to four reactions or
1095 steps away. **(2)** Description of reactions in the 5-FU metabolic neighborhood including up to
1096 four reactions or steps away.
1097

1098 **Table S3. NICEdrug score between all molecules with reactive site of statins in NICEdrug.ch,**
1099 **related to Figure 5.**
1100 Matrix of NICEdrug score between each pair of the whole set of 254 molecules in NICEdrug.ch
1101 with reactive site of statins.
1102

1103 **Table S4. Description of nine drugs candidates for repurposing to replace statins based on**
1104 **NICEdrug.ch, related to Figure 5.**
1105 These drugs can act as competitive inhibitors of HMG-CoA reductase like statins.
1106

1107 **Table S5. Essential genes or enzymes and linked metabolites in liver-stage *Plasmodium* and**
1108 **a human cell, related to Figure 6.**
1109 **(A)** List of essential genes and associated reactions in liver-stage *Plasmodium*, as obtained
1110 from the study (Stanway et al., 2019) **(B)** List of essential genes and associated reactions in a

1111 human cell, as obtained from the study (Wang et al., 2015) **(C)** List of metabolites linked to
1112 essential genes in liver-stage *Plasmodium*. **(D)** List of metabolites linked to essential genes in
1113 a human cell.
1114
1115 **Table S6. Description of drugs, prodrugs, metabolites and enzymes analyzed in the study of**
1116 **malaria, related to Figure 6**
1117 **(A)** NICEdrug druggability analysis of essential genes or enzymes in liver-stage *Plasmodium*:
1118 all drugs sharing reactive-site centric similarity with the *Plasmodium* metabolites and
1119 comparison with human metabolites. **(B)** NICEdrug druggability analysis of essential genes or
1120 enzymes in liver-stage *Plasmodium*: all prodrugs (up to three steps away of 346 drugs) sharing
1121 reactive-site centric similarity with the *Plasmodium* metabolites and comparison with human
1122 metabolites. **(C)** Description of drugs and prodrugs identified in the malaria analysis with
1123 NICEdrug.ch and validated in the study by (Antonova-Koch et al., 2018) along with their similar
1124 *Plasmodium* metabolite and human metabolite.
1125
1126 **Table S7. Hijacked human enzymes by SARS-CoV-2, and drugs and food-based compounds**
1127 **that can inhibit them based on the NICEdrug score, related to Figure 7.**
1128 **(A)** Hijacked human proteins by SARS-CoV-2 as identified by (Gordon et al., 2020) with an
1129 annotated enzymatic function (E.C. number), also called here "SARS-CoV-2 hijacked
1130 enzymes". **(B)** NICEdrug druggability report for SARS-CoV-2 hijacked enzymes including all
1131 NICEdrug small molecules. **(C)** Best candidate drugs against COVID-19: NICEdrug druggability
1132 report for SARS-CoV-2 hijacked enzymes including drugs with NICEdrug score above 0.5
1133 compared to the native human substrate. **(D)** Summary of NICEdrug best candidate drugs
1134 against COVID-19 and their classification according to the drug category in the KEGG
1135 database. **(E)** NICEdrug druggability report of SARS-CoV-2 hijacked enzymes including
1136 prodrugs (up to three steps away of any NICEdrug small molecule) with NICEdrug score above
1137 0.5 compared to the native human substrate. **(F)** Best candidate food-based molecules
1138 against COVID-19: NICEdrug druggability report of SARS-CoV-2 hijacked enzymes including
1139 food-based molecules with NICEdrug score above 0.5 compared to the native human
1140 substrate. **(G)** Summary of the NICEdrug best candidate food-based molecules against COVID-
1141 19 and their classification according to the fooDB source.
1142

1143 **Table S8. NICEdrug analysis of inhibitory mechanisms of currently used anti SARS-CoV-2**
1144 **drugs, related to Figure 7.**

1145 **(A)** All drug molecules and **(B)** prodrugs in NICEdrug.ch sharing reactive site with the native
1146 substrates of the human enzyme HDAC2 and their NICEdrug score with this substrate. **(C)** All
1147 molecules cataloged in fooDB sharing reactive site with the native substrates of the human
1148 enzyme HDAC2 and their NICEdrug score with this substrate. **(D)** All drug molecules and **(E)**
1149 prodrug molecules in NICEdrug.ch sharing reactive site with the native substrates of the
1150 human enzyme ACE2 and their NICEdrug score with this substrate. **(F)** All molecules cataloged
1151 in fooDB sharing reactive site with the native substrates of the human enzyme ACE2 and their
1152 NICEdrug score with this substrate. **(G)** All molecules in NICEdrug.ch or cataloged in fooDB
1153 sharing reactive site with the native substrates of the human enzyme DNA-directed RNA
1154 polymerase and their NICEdrug score with this substrate.

1155

References

Abdel-Atty, M.M., Farag, N.A., Kassab, S.E., Serya, R.A.T., and Abouzid, K.A.M. (2014). Design, synthesis, 3D pharmacophore, QSAR, and docking studies of carboxylic acid derivatives as Histone Deacetylase inhibitors and cytotoxic agents. Bioorganic Chem. *57*, 65–82.

Alakwaa, F.M. (2020). Repurposing Didanosine as a Potential Treatment for COVID-19 Using Single-Cell RNA Sequencing Data. MSystems *5*.

Antonova-Koch, Y., Meister, S., Abraham, M., Luth, M.R., Ottilie, S., Lukens, A.K., Sakata-Kato, T., Vanaerschot, M., Owen, E., Jado, J.C., et al. (2018). Open-source discovery of chemical leads for next-generation chemoprotective antimalarials. Science *362*, eaat9446.

Ariens, E.J. (2012). Molecular Pharmacology V3: The Model of Action of Biology Active Compounds (Elsevier).

Bielas, J.H., Schmitt, M.W., Icreverzi, A., Ericson, N.G., and Loeb, L.A. (2009). Molecularly Evolved Thymidylate Synthase Inhibits 5-Fluorodeoxyuridine Toxicity in Human Hematopoietic Cells. Hum. Gene Ther. *20*, 1703–1707.

Brilisauer, K., Rapp, J., Rath, P., Schöllhorn, A., Bleul, L., Weiß, E., Stahl, M., Grond, S., and Forchhammer, K. (2019). Cyanobacterial antimetabolite 7-deoxy-sedoheptulose blocks the shikimate pathway to inhibit the growth of prototrophic organisms. Nat. Commun. *10*, 545.

Brunk, E., Sahoo, S., Zielinski, D.C., Altunkaya, A., Dräger, A., Mih, N., Gatto, F., Nilsson, A., Gonzalez, G.A.P., Aurich, M.K., et al. (2018). Recon3D: A Resource Enabling A Three-Dimensional View of Gene Variation in Human Metabolism. Nat. Biotechnol. *36*, 272–281.

Bushell, E., Gomes, A.R., Sanderson, T., Anar, B., Girling, G., Herd, C., Metcalf, T., Modrzynska, K., Schwach, F., Martin, R.E., et al. (2017). Functional Profiling of a Plasmodium Genome Reveals an Abundance of Essential Genes. Cell *170*, 260-272.e8.

Cava, C., Bertoli, G., and Castiglioni, I. (2020). In Silico Discovery of Candidate Drugs against Covid-19. Viruses *12*, 404.

Croft, D., O'Kelly, G., Wu, G., Haw, R., Gillespie, M., Matthews, L., Caudy, M., Garapati, P., Gopinath, G., Jassal, B., et al. (2011). Reactome: a database of reactions, pathways and biological processes. Nucleic Acids Res. *39*, D691–D697.

Díaz-Quiroz, D.C., Cardona-Félix, C.S., Viveros-Ceballos, J.L., Reyes-González, M.A., Bolívar, F., Ordoñez, M., and Escalante, A. (2018). Synthesis, biological activity and molecular modelling studies of shikimic acid derivatives as inhibitors of the shikimate dehydrogenase enzyme of Escherichia coli. J. Enzyme Inhib. Med. Chem. *33*, 397–404.

Dong, E., Du, H., and Gardner, L. (2020). An interactive web-based dashboard to track COVID-19 in real time. Lancet Infect. Dis. *20*, 533–534.

Endo, A., and Hasumi, K. (1993). HMG-CoA reductase inhibitors. Nat. Prod. Rep. *10*, 541.

Finley, S.D., Broadbelt, L.J., and Hatzimanikatis, V. (2009). Computational Framework for Predictive Biodegradation. Biotechnol. Bioeng. *104*, 1086–1097.

Ghattas, M.A., Raslan, N., Sadeq, A., Al Sorkhy, M., and Atatreh, N. (2016). Druggability analysis and classification of protein tyrosine phosphatase active sites. Drug Des. Devel. Ther. *10*, 3197–3209.

Gordon, D.E., Jang, G.M., Bouhaddou, M., Xu, J., Obernier, K., White, K.M., O'Meara, M.J., Rezelj, V.V., Guo, J.Z., Swaney, D.L., et al. (2020). A SARS-CoV-2 protein interaction map reveals targets for drug repurposing. Nature.

Guengerich, F.P. (2011). Mechanisms of Drug Toxicity and Relevance to Pharmaceutical Development. Drug Metab. Pharmacokinet. *26*, 3–14.

Hadadi, N., and Hatzimanikatis, V. (2015). Design of computational retrobiosynthesis tools for the design of de novo synthetic pathways. Curr. Opin. Chem. Biol. *28*, 99–104.

Hadadi, N., Hafner, J., Shajkofci, A., Zisaki, A., and Hatzimanikatis, V. (2016). ATLAS of Biochemistry: A Repository of All Possible Biochemical Reactions for Synthetic Biology and Metabolic Engineering Studies. ACS Synth. Biol. *5*, 1155–1166.

Hadadi, N., MohammadiPeyhani, H., Miskovic, L., Seijo, M., and Hatzimanikatis, V. (2019). Enzyme annotation for orphan and novel reactions using knowledge of substrate reactive sites. Proc. Natl. Acad. Sci. 201818877.

Hafner, J., MohammadiPeyhani, H., Sveshnikova, A., Scheidegger, A., and Hatzimanikatis, V. (2020). Updated ATLAS of Biochemistry with New Metabolites and Improved Enzyme Prediction Power. ACS Synth. Biol. *9*, 1479–1482.

Hatzimanikatis, V., Li, C., Ionita, J.A., Henry, C.S., Jankowski, M.D., and Broadbelt, L.J. (2005). Exploring the diversity of complex metabolic networks. Bioinformatics *21*, 1603–1609.

Henry, C.S., Broadbelt, L.J., and Hatzimanikatis, V. (2010). Discovery and analysis of novel metabolic pathways for the biosynthesis of industrial chemicals: 3-hydroxypropanoate. Biotechnol. Bioeng. n/a-n/a.

Istvan, E.S. (2001). Structural Mechanism for Statin Inhibition of HMG-CoA Reductase. Science *292*, 1160–1164.

Jankowski, M.D., Henry, C.S., Broadbelt, L.J., and Hatzimanikatis, V. (2008). Group Contribution Method for Thermodynamic Analysis of Complex Metabolic Networks. Biophys. J. *95*, 1487–1499.

Jarvis, A., and Ouvry, G. (2019). Essential ingredients for rational drug design. Bioorg. Med. Chem. Lett. *29*, 126674.

Javdan, B., Lopez, J.G., Chankhamjon, P., Lee, Y.-C.J., Hull, R., Wu, Q., Wang, X., Chatterjee, S., and Donia, M.S. (2020). Personalized Mapping of Drug Metabolism by the Human Gut Microbiome. Cell.

Jeon, S., Ko, M., Lee, J., Choi, I., Byun, S.Y., Park, S., Shum, D., and Kim, S. (2020). Identification of antiviral drug candidates against SARS-CoV-2 from FDA-approved drugs. Antimicrob. Agents Chemother. AAC.00819-20.

Jiang, S.-Y., Li, H., Tang, J.-J., Wang, J., Luo, J., Liu, B., Wang, J.-K., Shi, X.-J., Cui, H.-W., Tang, J., et al. (2018). Discovery of a potent HMG-CoA reductase degrader that eliminates statin-induced reductase accumulation and lowers cholesterol. Nat. Commun. *9*, 5138.

Kim, H.M., Shin, D.R., Yoo, O.J., Lee, H., and Lee, J.-O. (2003). Crystal structure of Drosophila angiotensin I-converting enzyme bound to captopril and lisinopril 1. FEBS Lett. *538*, 65–70.

Ko, M., Chang, S.Y., Byun, S.Y., Choi, I., d'Alexandry d'Orengiani, A.-L.P.H., Shum, D., Min, J.-Y., and Windisch, M.P. (2020). Screening of FDA-approved drugs using a MERS-CoV clinical isolate from South Korea identifies potential therapeutic options for COVID-19. BioRxiv 2020.02.25.965582.

Kobayakawa, M., and Kojima, Y. (2011). Tegafur/gimeracil/oteracil (S-1) approved for the treatment of advanced gastric cancer in adults when given in combination with cisplatin: a review comparing it with other fluoropyrimidine-based therapies. OncoTargets Ther. *4*, 193–201.

Kong, W., Wei, J., Abidi, P., Lin, M., Inaba, S., Li, C., Wang, Y., Wang, Z., Si, S., Pan, H., et al. (2004). Berberine is a novel cholesterol-lowering drug working through a unique mechanism distinct from statins. Nat. Med. *10*, 1344–1351.

Krauß, J., and Bracher, F. (2018). Pharmacokinetic Enhancers (Boosters)—Escort for Drugs against Degrading Enzymes and Beyond. Sci. Pharm. *86*, 43.

Levenshtein, V.I. (1966). Binary Codes Capable of Correcting Deletions, Insertions and Reversals. Sov. Phys. Dokl. *10*, 707.

Li, S., Li, Q., Li, Y., Li, L., Tian, H., and Sun, X. (2015). Acetyl-L-Carnitine in the Treatment of Peripheral Neuropathic Pain: A Systematic Review and Meta-Analysis of Randomized Controlled Trials. PLoS ONE *10*.

Lim, N.H., Kashiwagi, M., Visse, R., Jones, J., Enghild, J.J., Brew, K., and Nagase, H. (2010). Reactive-site mutants of N-TIMP-3 that selectively inhibit ADAMTS-4 and ADAMTS-5: biological and structural implications. Biochem. J. *431*, 113–122.

Lipinski, C.A., Lombardo, F., Dominy, B.W., and Feeney, P.J. (2001). Experimental and computational approaches to estimate solubility and permeability in drug discovery and development settings1PII of original article: S0169-409X(96)00423-1. The article was originally published in Advanced Drug Delivery Reviews 23 (1997) 3–25.1. Adv. Drug Deliv. Rev. *46*, 3–26.

Lodigiani, C., Iapichino, G., Carenzo, L., Cecconi, M., Ferrazzi, P., Sebastian, T., Kucher, N., Studt, J.-D., Sacco, C., Alexia, B., et al. (2020). Venous and arterial thromboembolic complications in COVID-19 patients admitted to an academic hospital in Milan, Italy. Thromb. Res. *191*, 9–14.

Longley, D.B., Harkin, D.P., and Johnston, P.G. (2003). 5-Fluorouracil: mechanisms of action and clinical strategies. Nat. Rev. Cancer *3*, 330–338.

Ma, W.W., Saif, M.W., El-Rayes, B.F., Fakih, M.G., Cartwright, T.H., Posey, J.A., King, T.R., von Borstel, R.W., and Bamat, M.K. (2017). Emergency use of uridine triacetate for the prevention and treatment of life-threatening 5-fluorouracil and capecitabine toxicity. Cancer *123*, 345–356.

Mahmoudian, M., and Rahimi-Moghaddam, P. (2009). The anti-cancer activity of noscapine: a review. Recent Patents Anticancer Drug Discov. *4*, 92–97.

Mårtensson, J., Gustafsson, J., and Larsson, A. (1989). A therapeutic trial with N-acetylcysteine in subjects with hereditary glutathione synthetase deficiency (5-oxoprolinuria). J. Inherit. Metab. Dis. *12*, 120–130.

Matsuda, R., Bi, C., Anguizola, J., Sobansky, M., Rodriquez, E., Badilla, J.V., Zheng, X., Hage, B., and Hage, D.S. (2014). STUDIES OF METABOLITE-PROTEIN INTERACTIONS: A REVIEW. J. Chromatogr. B Analyt. Technol. Biomed. Life. Sci. *966*, 48.

Mulhaupt, F., Matter, C.M., Kwak, B.R., Pelli, G., Veillard, N.R., Burger, F., Graber, P., Lüscher, T.F., and Mach, F. (2003). Statins (HMG-CoA reductase inhibitors) reduce CD40 expression in human vascular cells. Cardiovasc. Res. *59*, 755–766.

O'Boyle, N.M., Banck, M., James, C.A., Morley, C., Vandermeersch, T., and Hutchison, G.R. (2011). Open Babel: An open chemical toolbox. J. Cheminformatics *3*, 33.

Papadatos, G., and Brown, N. (2013). In silico applications of bioisosterism in contemporary medicinal chemistry practice. Wiley Interdiscip. Rev. Comput. Mol. Sci. *3*, 339–354.

Park, Y.-J., Walls, A.C., Wang, Z., Sauer, M.M., Li, W., Tortorici, M.A., Bosch, B.-J., DiMaio, F., and Veesler, D. (2019). Structures of MERS-CoV spike glycoprotein in complex with sialoside attachment receptors. Nat. Struct. Mol. Biol. *26*, 1151–1157.

Pornputtapong, N., Nookaew, I., and Nielsen, J. (2015). Human metabolic atlas: an online resource for human metabolism. Database J. Biol. Databases Curation *2015*.

Rajesh, A., and International, C. (2011). Medicinal plant biotechnology (Cambridge, MA: CABI).

Robertson, J.G. (2005). Mechanistic Basis of Enzyme-Targeted Drugs. Biochemistry *44*, 5561–5571.

Robinson, J.L., Kocabaş, P., Wang, H., Cholley, P.-E., Cook, D., Nilsson, A., Anton, M., Ferreira, R., Domenzain, I., Billa, V., et al. (2020). An atlas of human metabolism. Sci. Signal. *13*, eaaz1482.

Sartorelli, A.C., and Johns, D.G. (2013). Antineoplastic and Immunosuppressive Agents: Part I (Springer Science & Business Media).

1298 Scalbert, A., Andres-Lacueva, C., Arita, M., Kroon, P., Manach, C., Urpi-Sarda, M., and Wishart,
1299 D. (2011). Databases on food phytochemicals and their health-promoting effects. J. Agric.
1300 Food Chem. *59*, 4331–4348.

1301 Schmidt, U., Struck, S., Gruening, B., Hossbach, J., Jaeger, I.S., Parol, R., Lindequist, U.,
1302 Teuscher, E., and Preissner, R. (2009). SuperToxic: a comprehensive database of toxic
1303 compounds. Nucleic Acids Res. *37*, D295–D299.

1304 Shilo, S., Rossman, H., and Segal, E. (2020). Axes of a revolution: challenges and promises of
1305 big data in healthcare. Nat. Med. *26*, 29–38.

1306 Soh, K.C., and Hatzimanikatis, V. (2010). DREAMS of metabolism. Trends Biotechnol. *28*, 501–
1307 508.

1308 Stanway, R.R., Bushell, E., Chiappino-Pepe, A., Roques, M., Sanderson, T., Franke-Fayard, B.,
1309 Caldelari, R., Golomingi, M., Nyonda, M., Pandey, V., et al. (2019). Genome-Scale Identification
1310 of Essential Metabolic Processes for Targeting the Plasmodium Liver Stage. Cell *179*, 1112-
1311 1128.e26.

1312 Stokes, J.M., Yang, K., Swanson, K., Jin, W., Cubillos-Ruiz, A., Donghia, N.M., MacNair, C.R.,
1313 French, S., Carfrae, L.A., Bloom-Ackerman, Z., et al. (2020). A Deep Learning Approach to
1314 Antibiotic Discovery. Cell *180*, 688-702.e13.

1315 Sushko, I., Salmina, E., Potemkin, V.A., Poda, G., and Tetko, I.V. (2012). ToxAlerts: a Web server
1316 of structural alerts for toxic chemicals and compounds with potential adverse reactions. J.
1317 Chem. Inf. Model. *52*, 2310–2316.

1318 Suzuki, M., Okuda, T., and Shiraki, K. (2006). Synergistic antiviral activity of acyclovir and
1319 vidarabine against herpes simplex virus types 1 and 2 and varicella-zoster virus. Antiviral Res.
1320 *72*, 157–161.

1321 Tanaka, Y., Sasaki, R., Fukui, F., Waki, H., Kawabata, T., Okazaki, M., Hasegawa, K., and Ando, S.
1322 (2004). Acetyl-L-carnitine supplementation restores decreased tissue carnitine levels and
1323 impaired lipid metabolism in aged rats. J. Lipid Res. *45*, 729–735.

1324 Testa, B. (2010). Principles of Drug Metabolism. In Burger's Medicinal Chemistry and Drug
1325 Discovery, (American Cancer Society), pp. 403–454.

1326 Thakkar, S., Chen, M., Fang, H., Liu, Z., Roberts, R., and Tong, W. (2018). The Liver Toxicity
1327 Knowledge Base (LKTB) and drug-induced liver injury (DILI) classification for assessment of
1328 human liver injury. Expert Rev. Gastroenterol. Hepatol. *12*, 31–38.

1329 Tokic, M., Hadadi, N., Ataman, M., Neves, D., Ebert, B.E., Blank, L.M., Miskovic, L., and
1330 Hatzimanikatis, V. (2018). Discovery and Evaluation of Biosynthetic Pathways for the
1331 Production of Five Methyl Ethyl Ketone Precursors. ACS Synth. Biol. *7*, 1858–1873.

1332 US Preventive Services Task Force (2016). Statin Use for the Primary Prevention of
1333 Cardiovascular Disease in Adults: US Preventive Services Task Force Recommendation
1334 Statement. JAMA *316*, 1997–2007.

Vamathevan, J., Clark, D., Czodrowski, P., Dunham, I., Ferran, E., Lee, G., Li, B., Madabhushi, A., Shah, P., Spitzer, M., et al. (2019). Applications of machine learning in drug discovery and development. Nat. Rev. Drug Discov. *18*, 463–477.

Verlinde, C.L., and Hol, W.G. (1994). Structure-based drug design: progress, results and challenges. Structure *2*, 577–587.

Wang, T., Birsoy, K., Hughes, N.W., Krupczak, K.M., Post, Y., Wei, J.J., Lander, E.S., and Sabatini, D.M. (2015). Identification and characterization of essential genes in the human genome. Science *350*, 1096.

Wassilew, S. (2005). Brivudin compared with famciclovir in the treatment of herpes zoster: effects in acute disease and chronic pain in immunocompetent patients. A randomized, double-blind, multinational study. J. Eur. Acad. Dermatol. Venereol. JEADV *19*, 47–55.

Weininger, D. (1988). SMILES, a chemical language and information system. 1. Introduction to methodology and encoding rules. J. Chem. Inf. Comput. Sci. *28*, 31–36.

Wishart, D.S., Feunang, Y.D., Marcu, A., Guo, A.C., Liang, K., Vázquez-Fresno, R., Sajed, T., Johnson, D., Li, C., Karu, N., et al. (2018). HMDB 4.0: the human metabolome database for 2018. Nucleic Acids Res. *46*, D608–D617.

Wong, C.H., Siah, K.W., and Lo, A.W. (2019). Estimation of clinical trial success rates and related parameters. Biostatistics *20*, 273–286.

World Health Organization (2018). World Malaria Report 2018.

Wu, Y., Si, F., Luo, L., Jing, F., Jiang, K., Zhou, J., and Yi, Q. (2018). The effect of melatonin on cardio fibrosis in juvenile rats with pressure overload and deregulation of HDACs. Korean J. Physiol. Pharmacol. Off. J. Korean Physiol. Soc. Korean Soc. Pharmacol. *22*, 607–616.

Yang, H., Li, J., Wu, Z., Li, W., Liu, G., and Tang, Y. (2017). Evaluation of Different Methods for Identification of Structural Alerts Using Chemical Ames Mutagenicity Data Set as a Benchmark. Chem Res Toxicol 10.

Zhang, X.-J., Qin, J.-J., Cheng, X., Shen, L., Zhao, Y.-C., Yuan, Y., Lei, F., Chen, M.-M., Yang, H., Bai, L., et al. (2020). In-hospital Use of Statins is Associated with a Reduced Risk of Mortality among Individuals with COVID-19. Cell Metab.

Figure 1

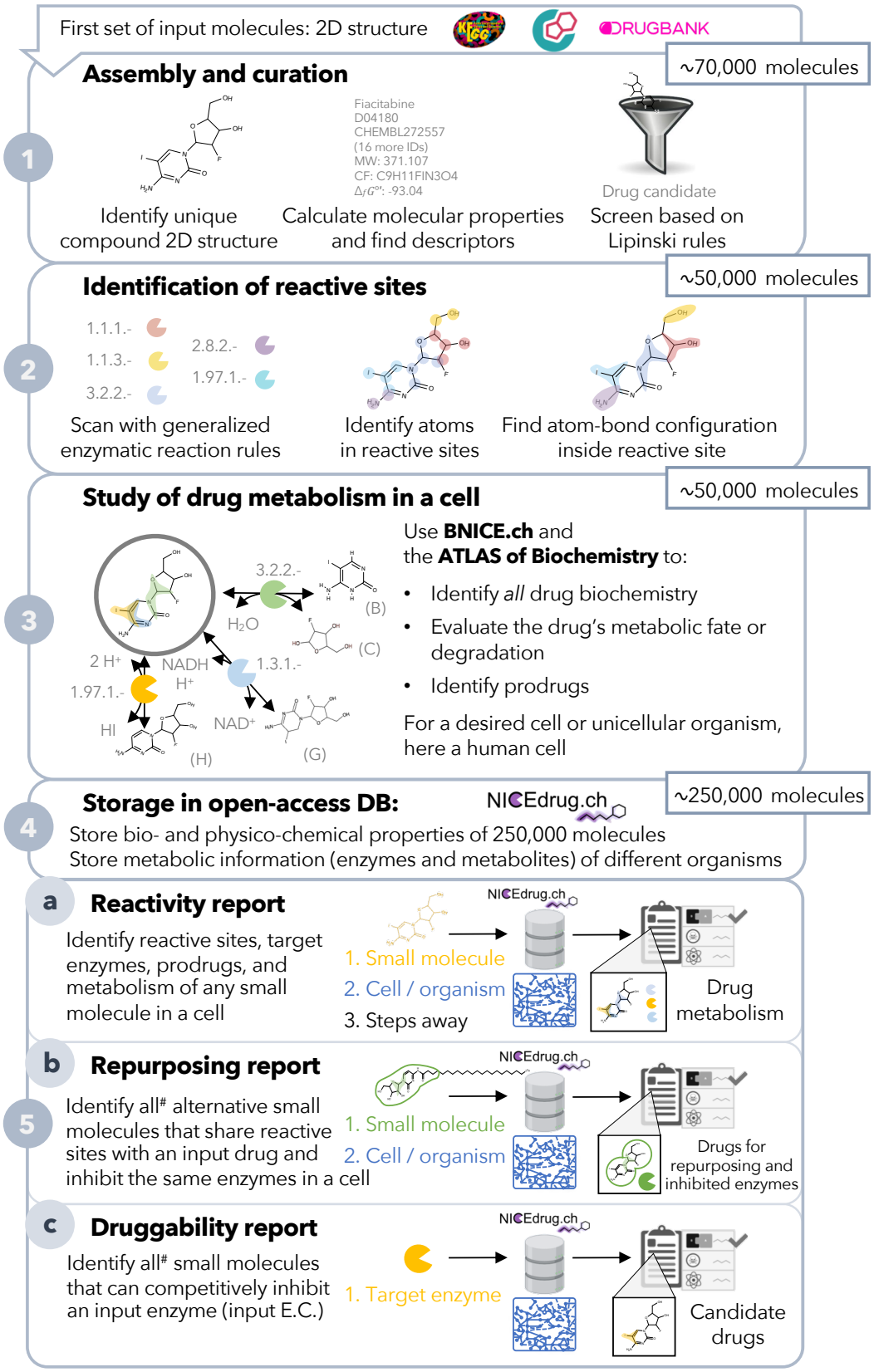

#among all small molecules in NICEdrug.ch, which will be continuously updated

Figure 2

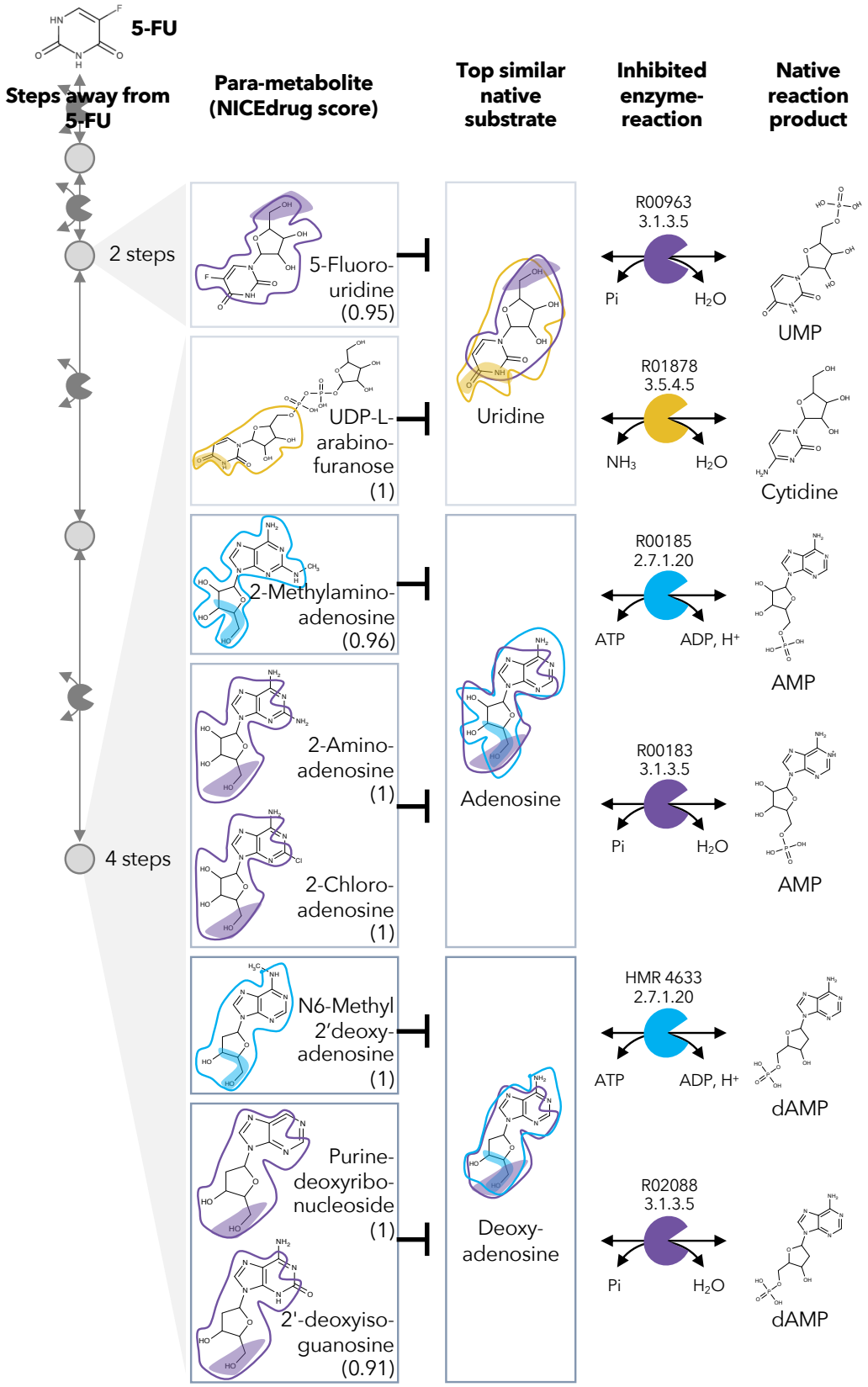
5-FU
Steps away from 5-FU
Para-metabolite (NICEdrug score)
Top similar native substrate
Inhibited enzyme-reaction
Native reaction product
2 steps
5-Fluoro-uridine (0.95)
UDP-L-arabino-furanose (1)
Uridine
R00963
3.1.3.5
Pi
H2O
UMP
R01878
3.5.4.5
NH3
H2O
Cytidine
4 steps
2-Methylamino-adenosine (0.96)
2-Amino-adenosine (1)
2-Chloro-adenosine (1)
Adenosine
R00185
2.7.1.20
ATP
ADP, H+
AMP
R00183
3.1.3.5
Pi
H2O
AMP
N6-Methyl 2'deoxy-adenosine (1)
Purine-deoxyribo-nucleoside (1)
2'-deoxyiso-guanosine (0.91)
Deoxy-adenosine
HMR 4633
2.7.1.20
ATP
ADP, H+
dAMP
R02088
3.1.3.5
Pi
H2O
dAMP

Figure 3

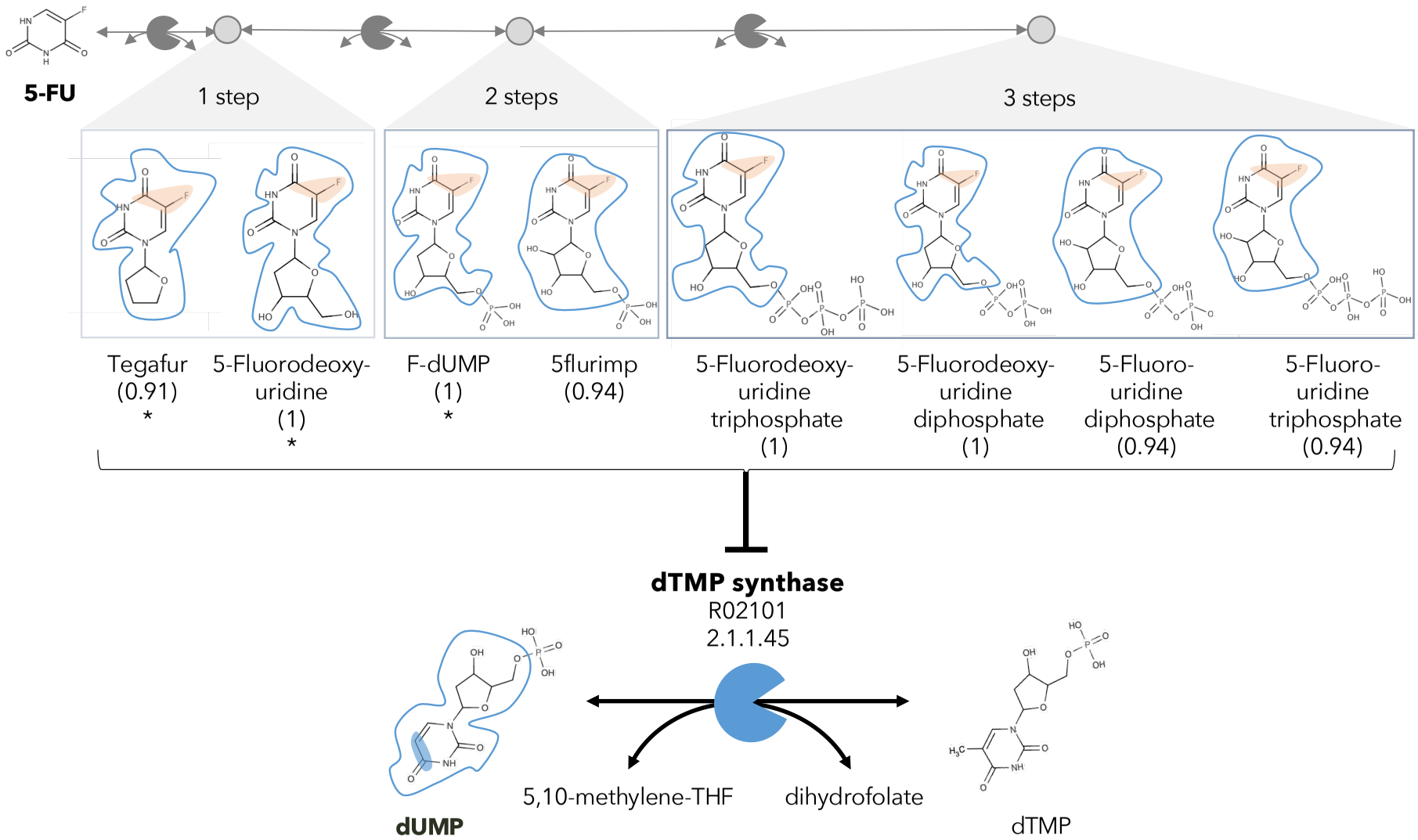
5-FU
1 step
2 steps
3 steps
Tegafur (0.91) *
5-Fluorodeoxy-uridine (1) *
F-dUMP (1) *
5flurimp (0.94)
5-Fluorodeoxy-uridine triphosphate (1)
5-Fluorodeoxy-uridine diphosphate (1)
5-Fluoro-uridine diphosphate (0.94)
5-Fluoro-uridine triphosphate (0.94)
dTMP synthase
R02101
2.1.1.45
dUMP
5,10-methylene-THF
dihydrofolate
dTMP

Figure 4

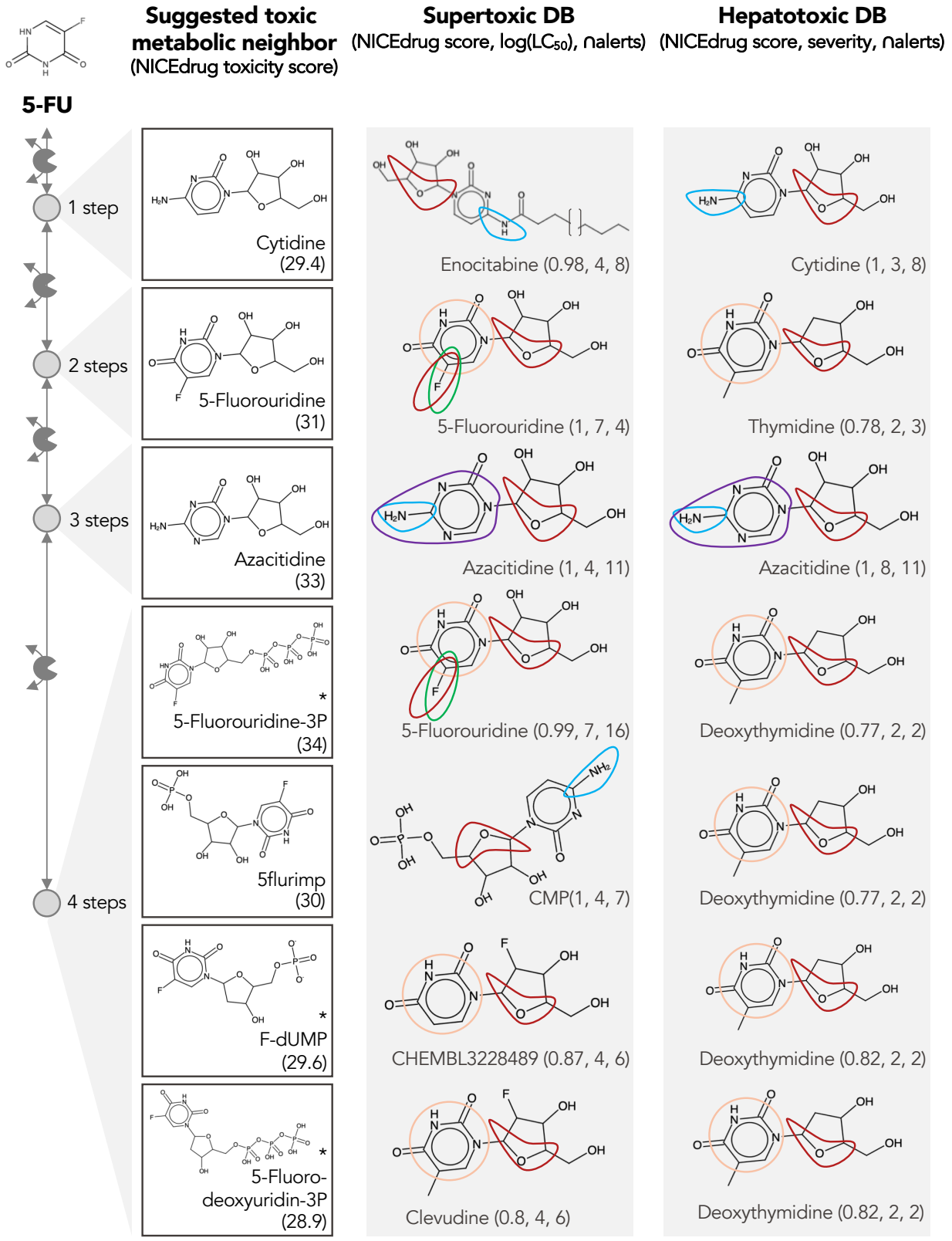

∩alerts: number of NICEdrug common toxic alerts
* Toxicity validated

- Genotoxic carcinogenicity, mutagenicity
- Non-biodegradability
- Acute aquatic toxicity
- Pyridinium-related toxicity
- Skin sensitization

Figure 5

A

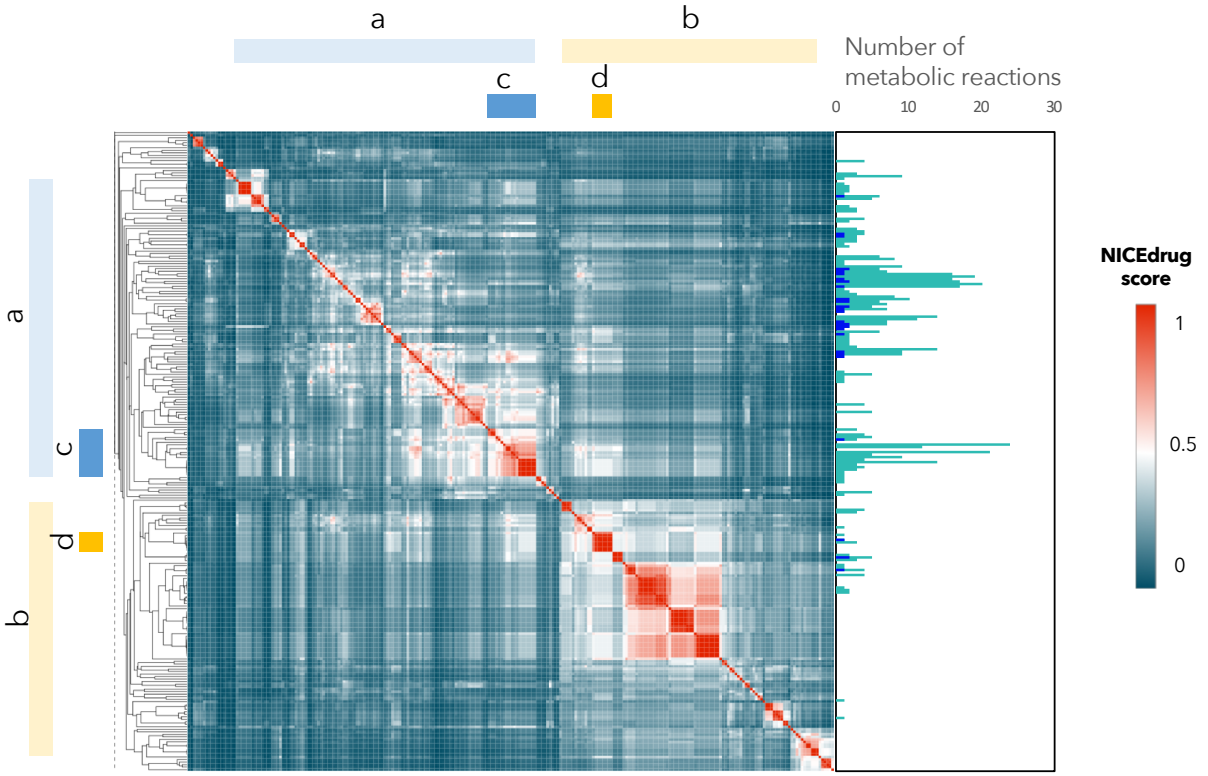
a
b
c
d
Number of metabolic reactions
0
10
20
30
NICEdrug score
1
0.5
0

B

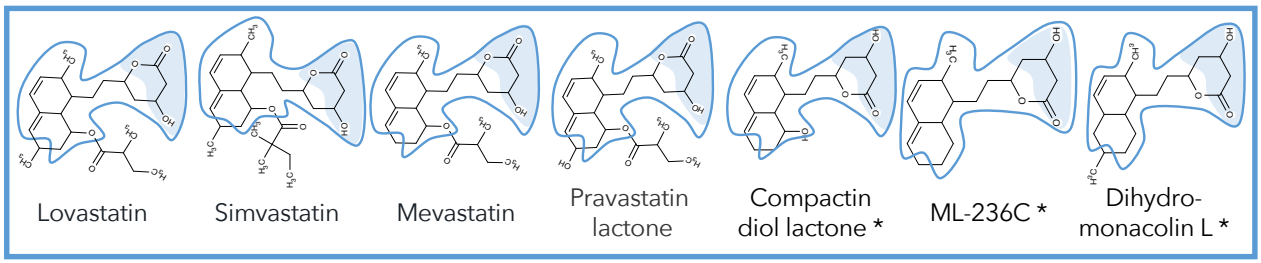
Lovastatin
Simvastatin
Mevastatin
Pravastatin lactone
Compactin diol lactone *
ML-236C *
Dihydro-monacolin L *

C

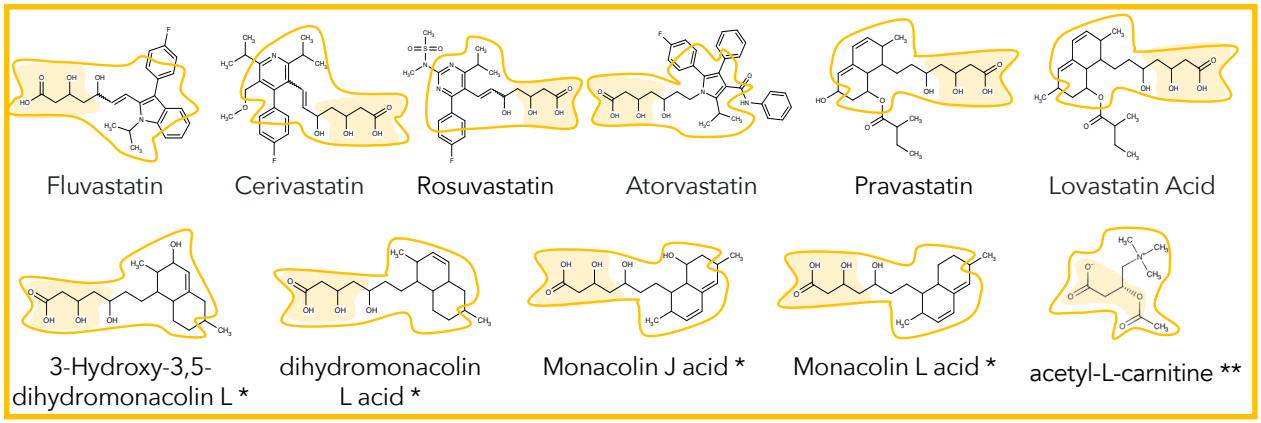
Fluvastatin
Cerivastatin
Rosuvastatin
Atorvastatin
Pravastatin
Lovastatin Acid
3-Hydroxy-3,5-dihydromonacolin L *
dihydromonacolin L acid *
Monacolin J acid *
Monacolin L acid *
acetyl-L-carnitine **

Figure 6

A

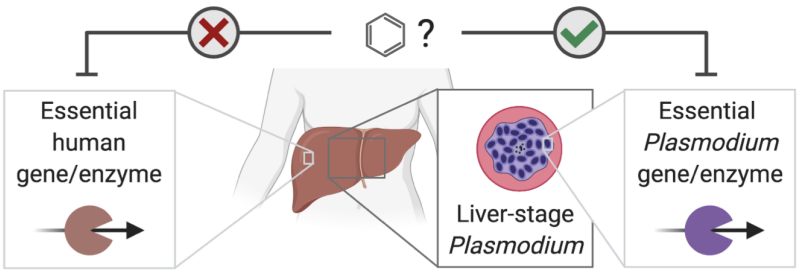
?
Essential human gene/enzyme
Liver-stage Plasmodium
Essential Plasmodium gene/enzyme

B

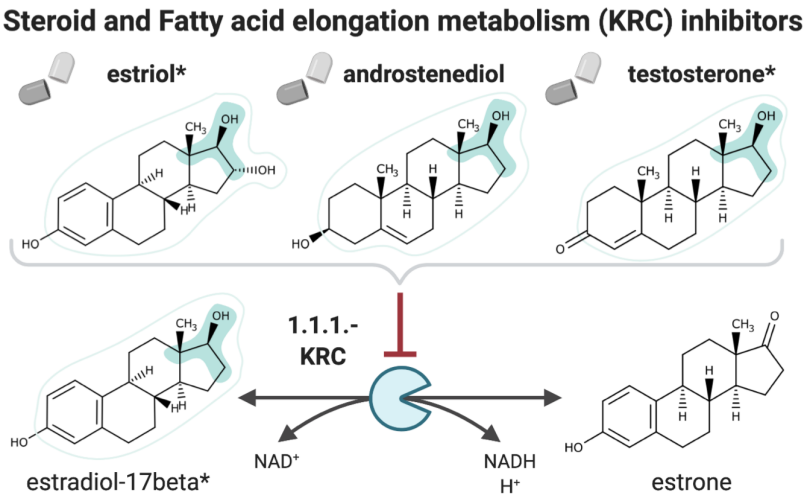
Steroid and Fatty acid elongation metabolism (KRC) inhibitors
estriol*
androstenediol
testosterone*
1.1.1.-
KRC
NAD+
NADH
H+
estradiol-17beta*
estrone

C

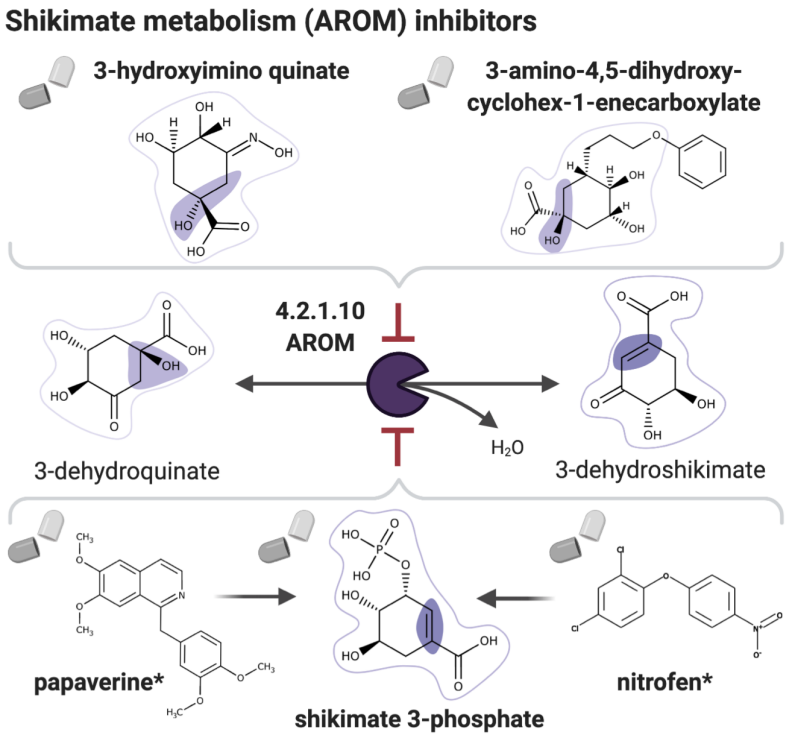
Shikimate metabolism (AROM) inhibitors
3-hydroxyimino quinate
3-amino-4,5-dihydroxy-cyclohex-1-enecarboxylate
4.2.1.10
AROM
H2O
3-dehydroquinate
3-dehydroshikimate
papaverine*
shikimate 3-phosphate
nitrofen*

Figure 7

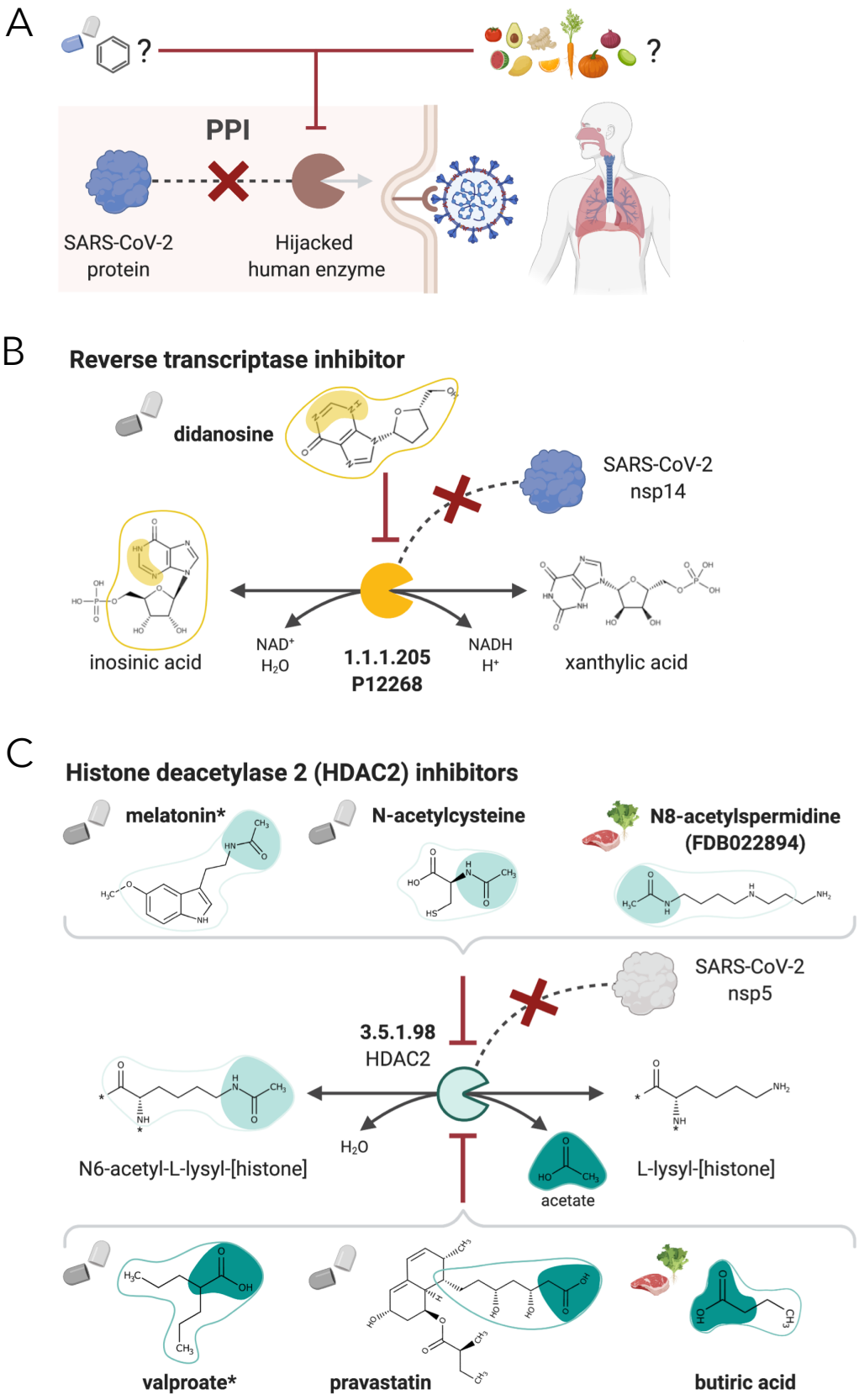
A
?
?
PPI
SARS-CoV-2
protein
Hijacked
human enzyme
B
Reverse transcriptase inhibitor
didanosine
SARS-CoV-2
nsp14
inosinic acid
NAD+
H2O
1.1.1.205
P12268
NADH
H+
xanthylic acid
C
Histone deacetylase 2 (HDAC2) inhibitors
melatonin*
N-acetylcysteine
N8-acetylspermidine
(FDB022894)
SARS-CoV-2
nsp5
3.5.1.98
HDAC2
N6-acetyl-L-lysyl-[histone]
H2O
acetate
L-lysyl-[histone]
valproate*
pravastatin
butiric acid

Figure S1

A

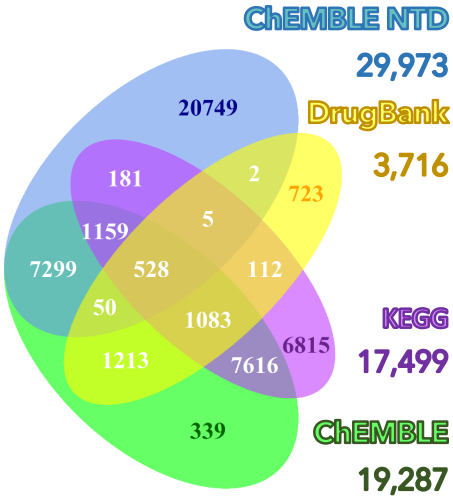
ChEMBLE NTD
29,973
DrugBank
3,716
KEGG
17,499
ChEMBLE
19,287
20749
181
2
723
5
1159
7299
528
112
50
1083
6815
1213
7616
339

B

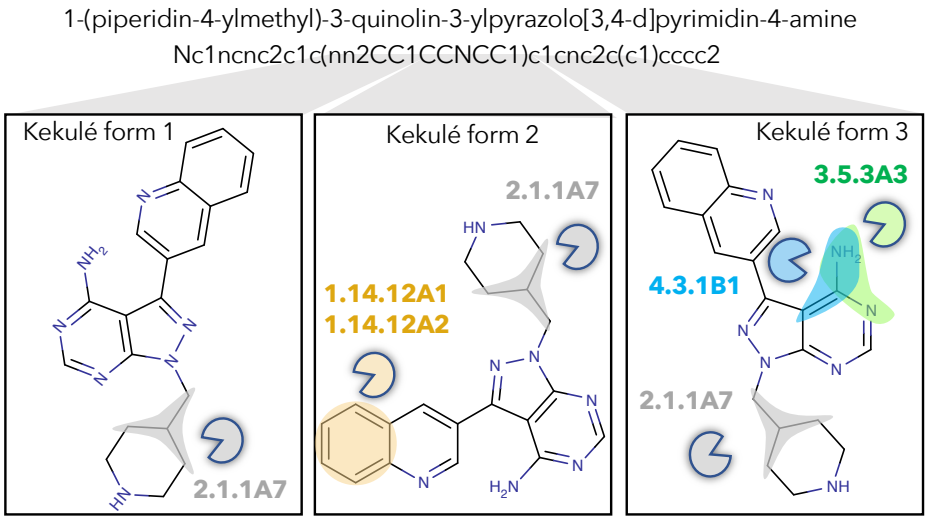
1-(piperidin-4-ylmethyl)-3-quinolin-3-ylpyrazolo[3,4-d]pyrimidin-4-amine
Nc1ncnc2c1c(nn2CC1CCNCC1)c1cnc2c(c1)cccc2
Kekulé form 1
2.1.1A7
Kekulé form 2
2.1.1A7
1.14.12A1
1.14.12A2
Kekulé form 3
3.5.3A3
4.3.1B1
2.1.1A7

Figure S2

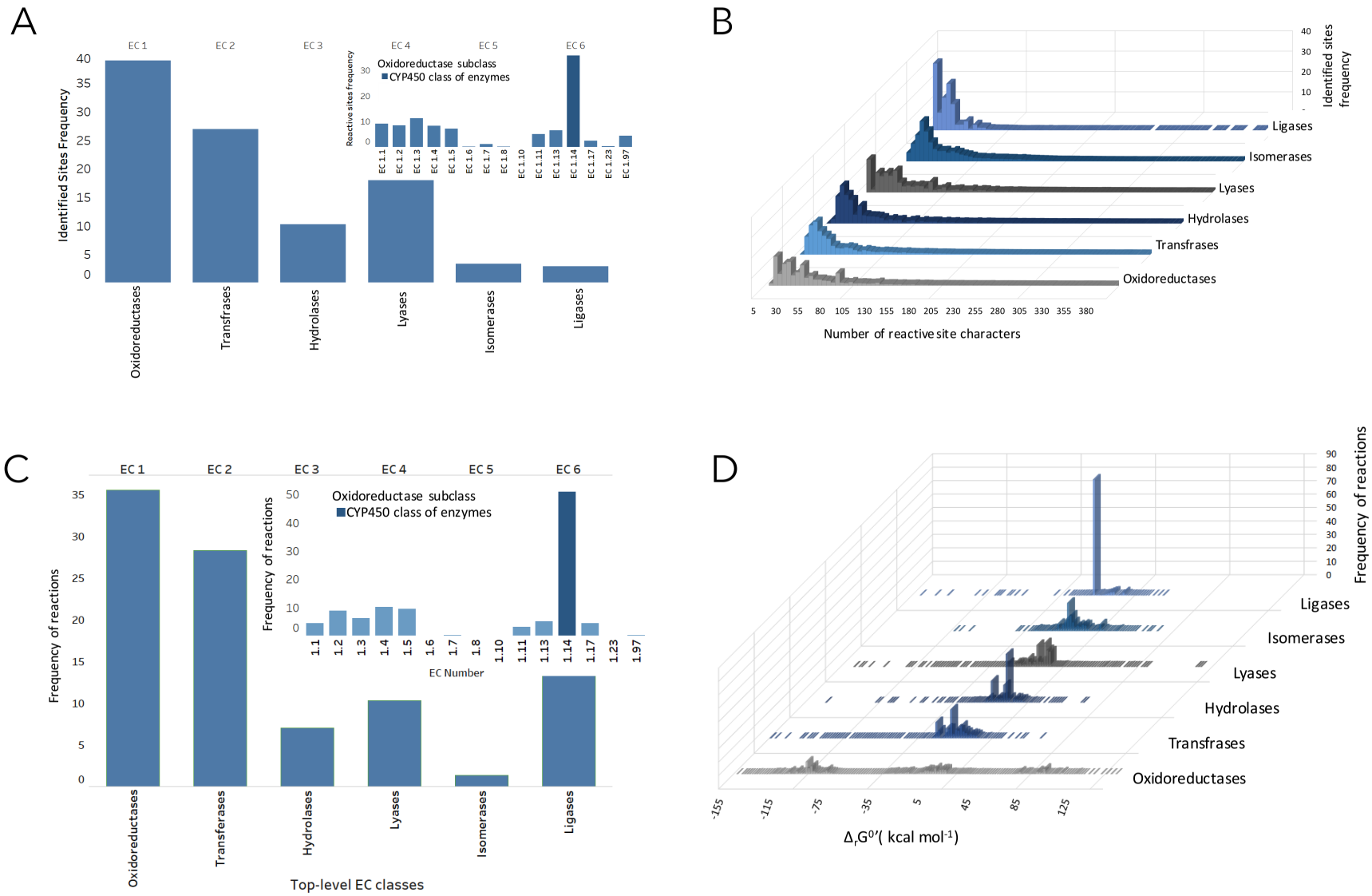
A
EC 1
EC 2
EC 3
EC 4
EC 5
EC 6
Identified Sites Frequency
Oxidoreductase subclass
CYP450 class of enzymes
Reactive sites frequency
Oxidoreductases
Transfrases
Hydrolases
Lyases
Isomerases
Ligases
B
Identified sites frequency
Ligases
Isomerases
Lyases
Hydrolases
Transfrases
Oxidoreductases
Number of reactive site characters
C
Frequency of reactions
Oxidoreductase subclass
CYP450 class of enzymes
EC Number
Oxidoreductases
Transferases
Hydrolases
Lyases
Isomerases
Ligases
Top-level EC classes
D
Frequency of reactions
Ligases
Isomerases
Lyases
Hydrolases
Transfrases
Oxidoreductases
$\Delta_r G^{0\prime}$(kcal mol^{-1})

Figure S3

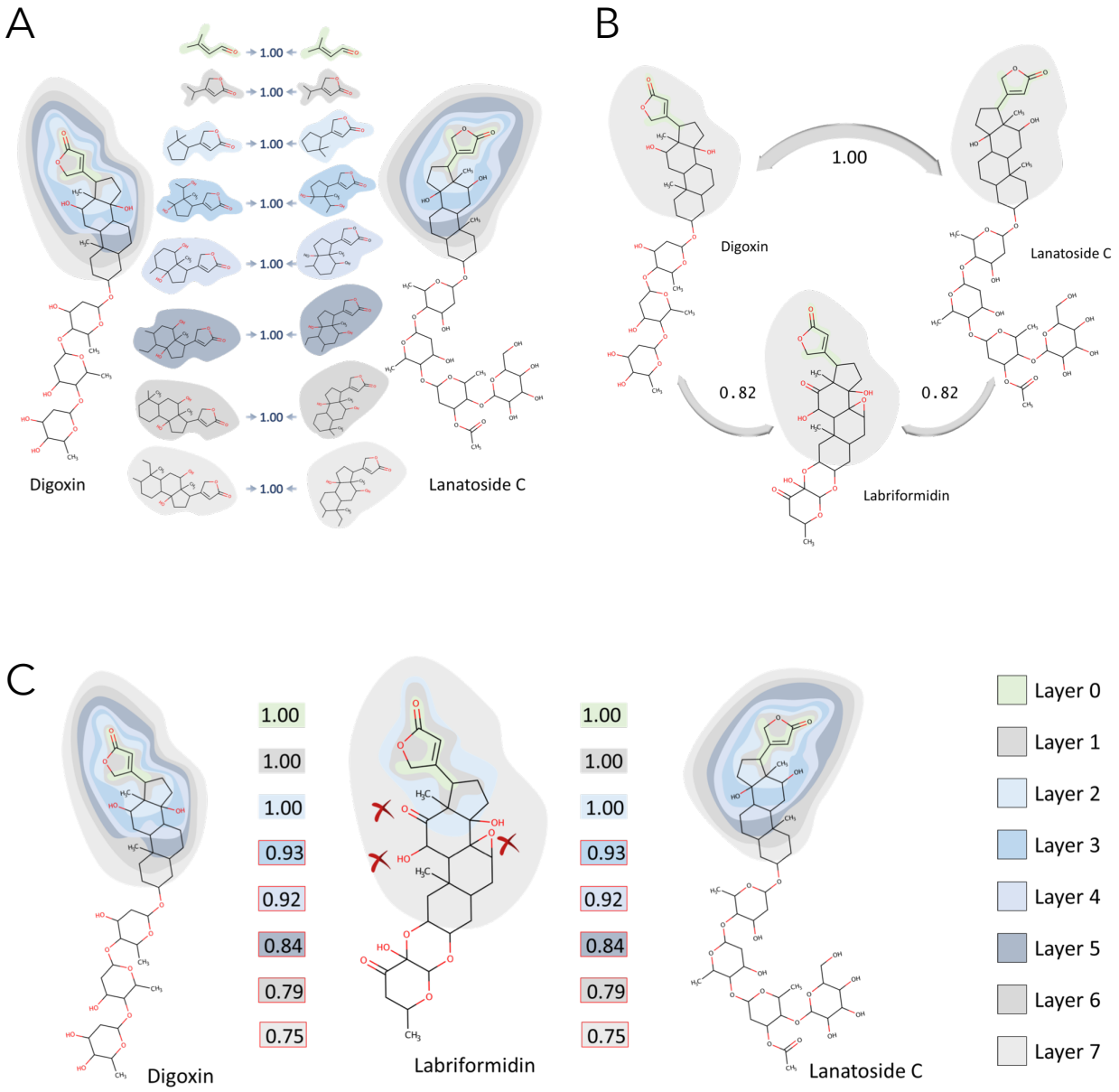
A
1.00
Digoxin
Lanatoside C
B
1.00
Digoxin
Lanatoside C
0.82
0.82
Labriformidin
C
1.00
1.00
1.00
0.93
0.92
0.84
0.79
0.75
Digoxin
Labriformidin
Lanatoside C
Layer 0
Layer 1
Layer 2
Layer 3
Layer 4
Layer 5
Layer 6
Layer 7

Figure S4

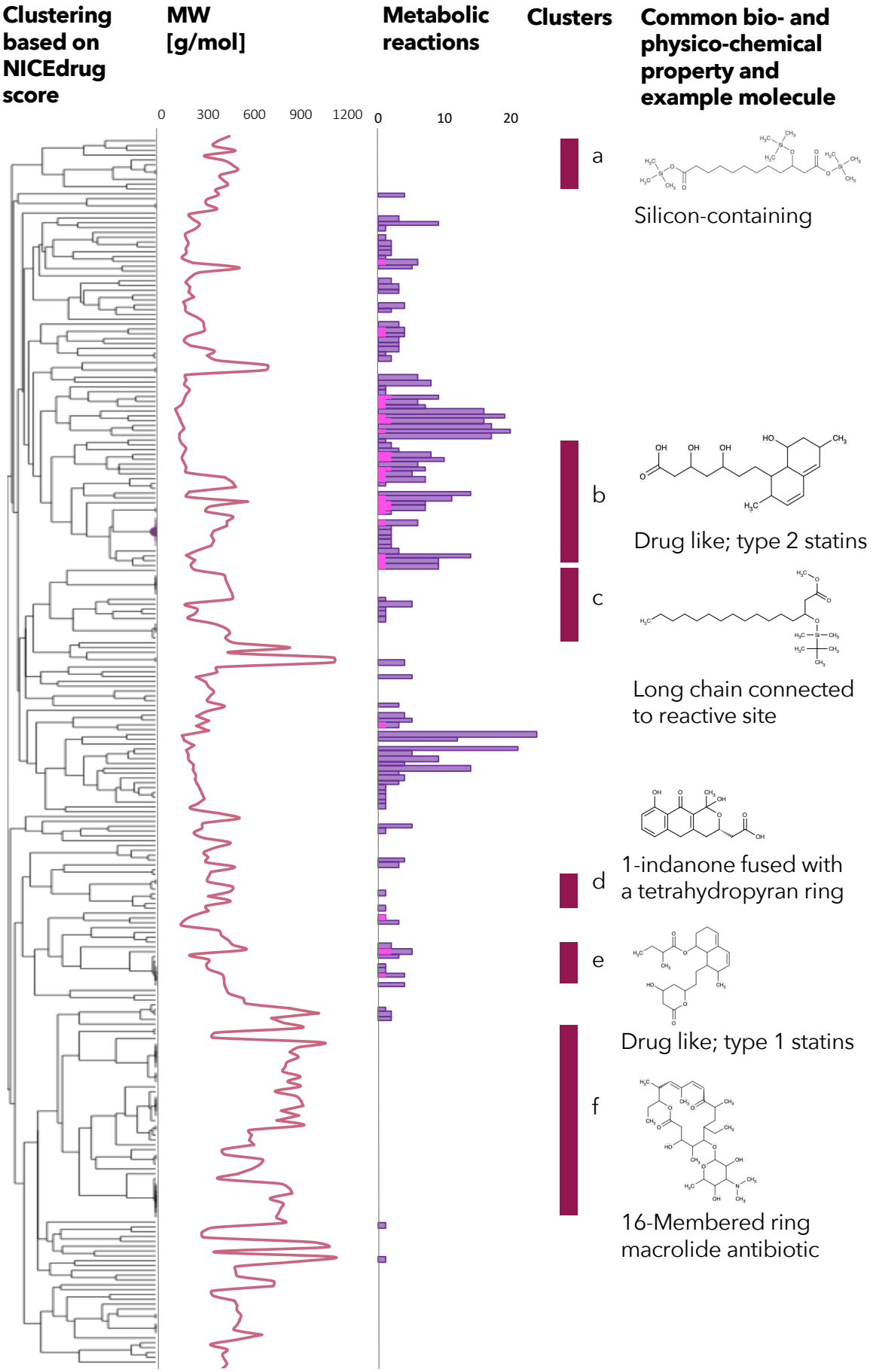
Clustering based on NICEdrug score
MW [g/mol]
0
300
600
900
1200
Metabolic reactions
0
10
20
Clusters
a
b
c
d
e
f
Common bio- and physico-chemical property and example molecule
Silicon-containing
Drug like; type 2 statins
Long chain connected to reactive site
1-indanone fused with a tetrahydropyran ring
Drug like; type 1 statins
16-Membered ring macrolide antibiotic

Figure S5

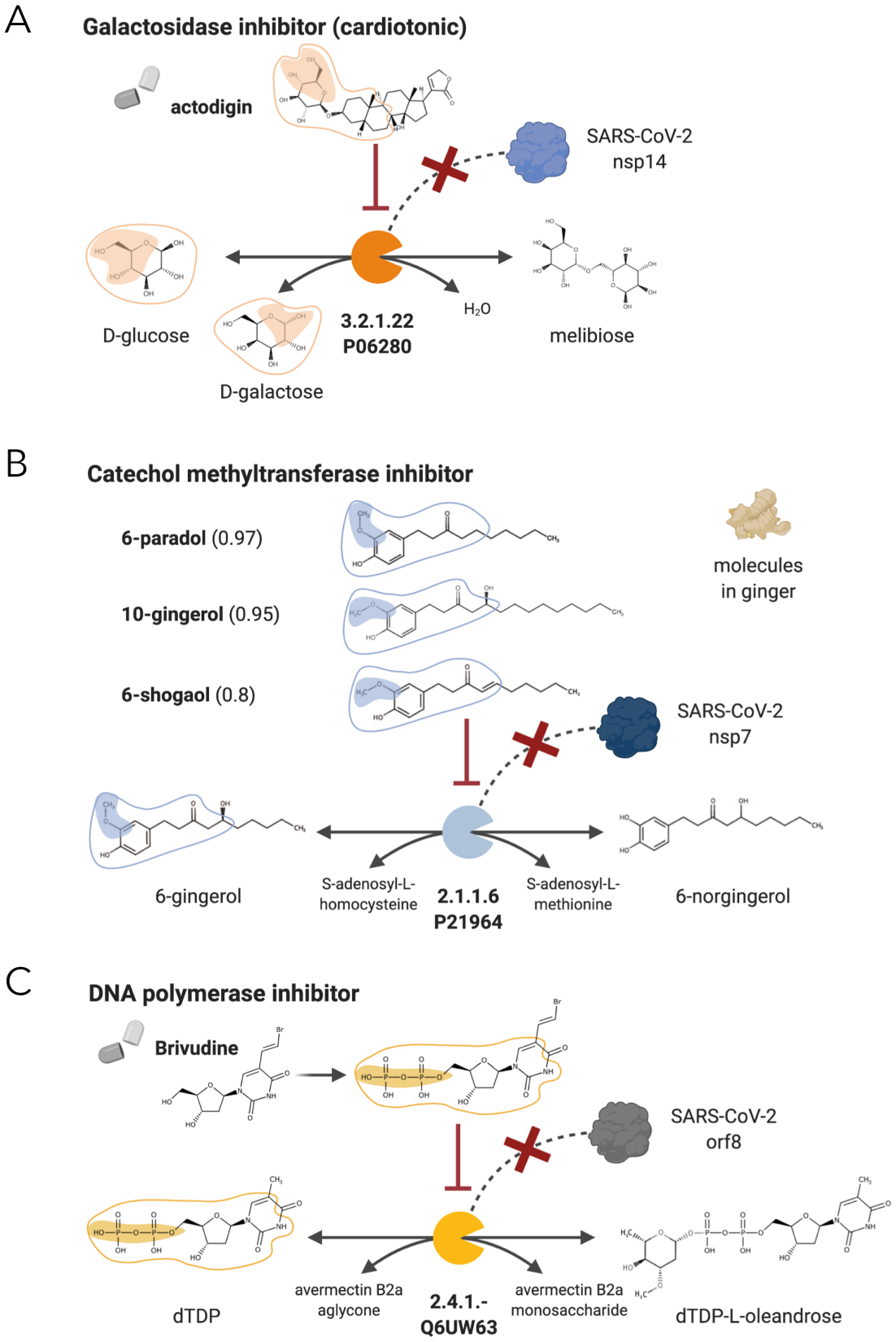
A
Galactosidase inhibitor (cardiotonic)
actodigin
SARS-CoV-2
nsp14
D-glucose
D-galactose
3.2.1.22
P06280
H2O
melibiose
B
Catechol methyltransferase inhibitor
6-paradol (0.97)
10-gingerol (0.95)
6-shogaol (0.8)
molecules
in ginger
SARS-CoV-2
nsp7
6-gingerol
S-adenosyl-L-
homocysteine
2.1.1.6
P21964
S-adenosyl-L-
methionine
6-norgingerol
C
DNA polymerase inhibitor
Brivudine
SARS-CoV-2
orf8
dTDP
avermectin B2a
aglycone
2.4.1.-
Q6UW63
avermectin B2a
monosaccharide
dTDP-L-oleandrose

Figure S6

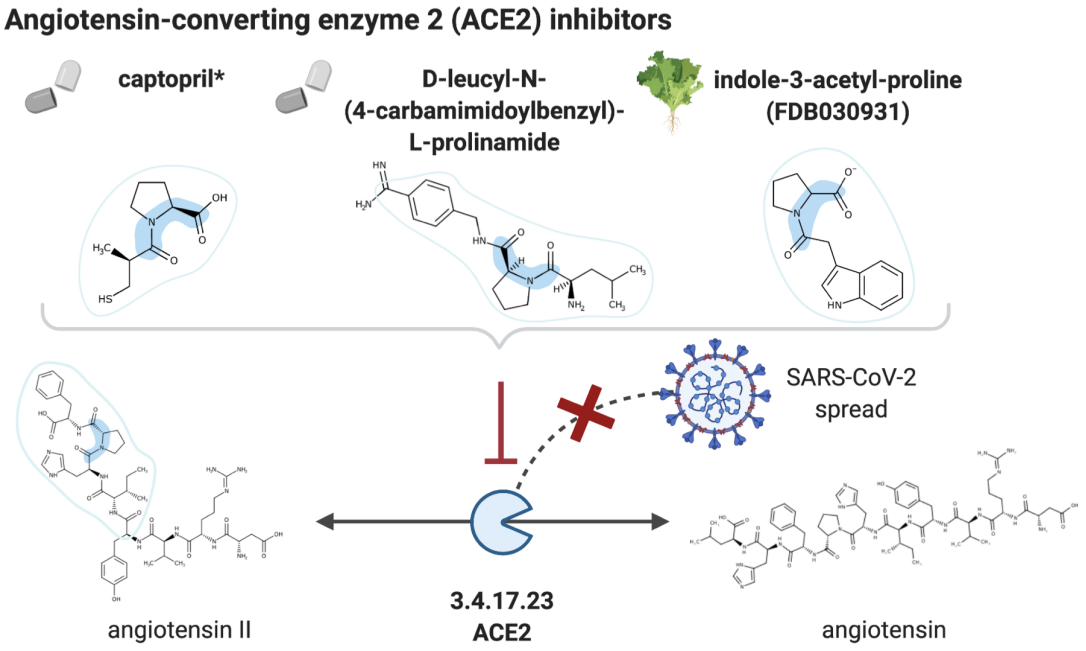
Angiotensin-converting enzyme 2 (ACE2) inhibitors
captopril*
D-leucyl-N-(4-carbamimidoylbenzyl)-L-prolinamide
indole-3-acetyl-proline (FDB030931)
SARS-CoV-2 spread
angiotensin II
3.4.17.23
ACE2
angiotensin